effects: a phase I clinical trial, J. Clin. Oncol. 19 (2001) 3422–3433.
[6] S.C. Hyde, K.W. Southern, U. Gileadi, E.M. Fitzjohn, K.A. Mofford, B.E. Waddell, H.C. Gooi, C.A. Goddard, K. Hannavy, S.E. Smyth, J.J. Egan, F.L. Sorgi, L. Huang, A.W. Cuthbert, M.J. Evans, W.H. Colledge, C.F. Higgins, A.K. Webb, D.R. Gill, Repeat administration of DNA/liposomes to the nasal epithelium of patents with cystic fiblosis, Gene Ther. 7 (2000) 1156–1165.
[7] J.S. Remy, A. Kichler, V. Mordvinov, F. Schuber, J.P. Behr, Targeted gene transfer into hepatoma cells with lipopolyamine-condensed DNA particles presenting galactose ligands: a stage toward artificial viruses, Proc. Natl. Acad. Sci. U. S. A. 92 (1995) 1744–1748.
[8] S. Kawakami, F. Yamashita, M. Nishikawa, Y. Takakura, M. Hashida, Asialoglycoprotein receptor-mediated gene transfer using novel galactosylated cationic liposomes, Biochem. Biophys. Res. Commun. 252 (1998) 78–83.
[9] P. Erbacher, M.T. Bousser, J. Raimond, M. Monsigny, P. Midoux, A.C. Roche, Gene transfer by DNA/glycosylated polylysine complex into human blood monocyte-derived macrophages, Hum. Gene Ther. 7 (1996) 721–729.
[10] S. Kawakami, A. Sato, M. Nishikawa, F. Yamashita, M. Hashida, Mannose receptor-mediated gene transfer into macrophages using novel mannosylated cationic liposomes, Gene Ther. 7 (2000) 292–299.
[11] D.T. Curiel, S. Agarwal, M.U. Romer, E. Wagner, M. Cotten, M.L. Birnstiel, R.C. Boucher, Gene transfer to respiratory epithelial cells via the receptor-mediated endocytosis pathway, Am. J. Respir. Cell Mol. Biol. 6 (1992) 247–252.
[12] L. Yano, M. Shimura, M. Taniguchi, Y. Hayashi, T. Suzuki, K. Hatake, F. Takaku, Y. Ishizaka, Improved gene transfer to neuroblastoma cells by a monoclonal antibody targeting RET, a receptor tyrosine kinase, Hum. Gene Ther. 11 (2000) 995–1004.
[13] T. Ohashi, S. Boggs, P. Robbins, A. Bahnson, K. Patrene, F. Wei, J. Wei, J. Li, L. Lucht, Y. Fei, S. Clark, M. Kimak, H. He, P. Mowery-Rushton, J.A. Barranger, Efficient transfer and sustained high expression of the human glucocerebrosidase gene in mice and their functional macrophages following transplantation of bone marrow transduced by a retroviral vector, Proc. Natl. Acad. Sci. U. S. A. 89 (1992) 11332–11336.
[14] D.B. Kohn, N. Sarver, Gene therapy for HIV-1 infection, Adv. Exp. Med. Biol. 394 (1996) 421–428.
[15] S. Kawakami, A. Sato, M. Yamada, F. Yamashita, M. Hashida, The effect of lipid composition on receptor-mediated in vivo gene transfection using mannosylated cationic liposomes in mice, STP Pharma Sci. 11 (2001) 117–120.
[16] K. Ogawara, S. Hasegawa, M. Nishikawa, Y. Takakura, M. Hashida, Pharmacokinetic evaluation of mannosylated bovine serum albumin as a liver cell-specific carrier: quantitative comparison with other hepatotropic ligands, J. Drug Target. 6 (1999) 349–360.
[17] G.R. Bartlett, Phosphorus assay in column chromatography, J. Biol. Chem. 234 (1959) 466–468.
[18] J.Y. Legendre, F.C. Szoka Jr., Cyclic amphipathic peptide–DNA complexes mediate high-efficiency transfection of adherent mammalian cells, Proc. Natl. Acad. Sci. U. S. A. 90 (1993) 893–897.
[19] S. Kawakami, S. Fumoto, M. Nishikawa, F. Yamashita, M. Hashida, In vivo gene delivery to the liver using novel galactosylated cationic liposomes, Pharm. Res. 17 (2000) 306–313.
[20] S. Fumoto, F. Nakadori, S. Kawakami, M. Nishikawa, F. Yamashita, M. Hashida, Analysis of hepatic disposition of galactosylated cationic liposome/plasmid DNA complexes in the rat perfused liver, Pharm. Res. 20 (2003) 1452–1459.
[21] K. Sambrook, E.F. Fritsch, T. Maniatis (Eds.), Molecular Cloning: A Laboratory Manual, 2nd edition, Cold Spring Harbor Laboratory Press, Plainview, NY, 1989.
[22] M. Nishikawa, T. Nakano, T. Okabe, N. Hamaguchi, Y. Yamasaki, Y. Takakura, F. Yamashita, M. Hashida, Residualizing indium-111-radiolabel for plasmid DNA and its application to tissue distribution studies, Bioconjug. Chem. 14 (2003) 955–961.
[23] C.A. Hoppe, Y.C. Lee, The binding and processing of mannose-bovine serum albumin derivatives by rabbit alveolar macrophages, J. Biol. Chem. 258 (1983) 14193–14199.
[24] M.E. Taylor, M.S. Leaning, J.A. Summerfield, Uptake and processing of glycoproteins by rat hepatic mannose receptor, Am. J. Physiol. 252 (1987) E690–E698.
[25] K. Kawabata, Y. Takakura, M. Hashida, The fate of plasmid DNA after intravenous injection in mice: involvement of scavenger receptors in its hepatic uptake, Pharm. Res. 12 (1995) 825–830.
[26] S. Kawakami, F. Yamashita, K. Nishida, J. Nakamura, M. Hashida, Glycosylated cationic liposomes for cell-selective gene delivery, Crit. Rev. Ther. Drug Carr. Syst. 19 (2002) 171–190.
[27] M. Nishikawa, H. Hirabayashi, Y. Takakura, M. Hashida, Design for cell-specific targeting of proteins utilizing sugar-recognition mechanism: effect of molecular weight of proteins on targeting efficiency, Pharm. Res. 12 (1995) 209–214.
[28] Y. Yabe, N. Kobayashi, T. Nishihashi, R. Takahashi, M. Nishikawa, Y. Takakura, M. Hashida, Prevention of neutrophil-mediated hepatic ischemia/reperfusion injury by superoxide dismutase and catalase derivatives, J. Pharmacol. Exp. Ther. 298 (2001) 894–899.
[29] F. Sakurai, T. Nishioka, H. Saito, T. Baba, A. Okuda, O. Matsumoto, T. Taga, F. Yamashita, Y. Takakura, M. Hashida, Interaction between DNA-cationic liposome complexes and erythrocytes is an important factor in systemic gene transfer via the intravenous route in mice: the role of the neutral helper lipid, Gene Ther. 8 (2001) 677–686.
[30] F. Sakurai, T. Nishioka, F. Yamashita, Y. Takakura, M. Hashida, Effects of erythrocytes and serum proteins on lung accumulation of lipoplexes containing cholesterol or DOPE as a helper lipid in the single-pass rat lung perfusion system, Eur. J. Pharm. Biopharm. 52 (2001) 165–172.

Significant Role of Liver Sinusoidal Endothelial Cells in Hepatic Uptake and Degradation of Naked Plasmid DNA After Intravenous Injection

Jin Hisazumi,[1] Naoki Kobayashi,[1] Makiya Nishikawa,[1] and Yoshinobu Takakura[1,2]

Received October 15, 2003; accepted March 14, 2004

Purpose. Uptake and degradation of naked plasmid DNA (pDNA) by liver sinusoidal endothelial cells (LSECs) were investigated.
Methods. Tissue distribution and intrahepatic localization were determined after an intravenous injection of ^{111}In- or ^{32}P-labeled pDNA into rats. Cellular uptake and degradation of fluorescein- or ^{32}P-labeled pDNA were evaluated using primary cultures of rat LSECs.
Results. Following intravenous injection, pDNA was rapidly eliminated from the circulation and taken up by the liver. Fractionation of liver-constituting cells by centrifugal elutriation revealed a major contribution of LSECs to the overall hepatic uptake of pDNA. Confocal microscopic study confirmed intracellular uptake of pDNA in cultured LSECs. Apparent cellular association of pDNA was similar at 37°C and 4°C. However, trichloroacetic acid (TCA) precipitation experiments showed the TCA-soluble radioactivity in the culture medium increased in an accumulative manner at 37°C. Involvement of a specific mechanism was demonstrated, as the uptake of pDNA was significantly inhibited by excess unlabeled pDNA and some polyanions (polyinosinic acid, dextran sulfate, heparin) but not by others (polycytidylic acid, dextran). These inhibitors also reduced the amount of TCA-soluble radioactivity in the culture medium.
Conclusion. These results suggest that LSECs efficiently ingested and rapidly degraded naked pDNA *in vivo* and *in vitro* and released the degradation products into the extracellular space.

KEY WORDS: degradation; liver sinusoidal endothelial cells; plasmid DNA; trichloroacetic acid; uptake.

INTRODUCTION

Plasmid DNA (pDNA), the simplest nonviral vector, is an important macromolecular agent for gene therapy or DNA vaccination (1,2). Though relatively low transfection efficiency is one of the main limiting factors of nonviral gene transfer strategies, pDNA has advantages in terms of its safety and versatility compared with viral vectors that potentially exhibit immunogenicity and undergo mutation thereby reacquiring the ability to produce infection.

In our previous study involving the *in vivo* disposition of pDNA, we demonstrated that pDNA is rapidly removed from the circulation, more quickly than its degradation by nucleases in the blood and other compartments, and taken up by the liver, predominantly by the liver nonparenchymal cells, after intravenous administration to mice (3). We also demonstrated the key role played by liver nonparenchymal cells in the hepatic uptake of pDNA in the single-pass rat liver perfusion system (4). In addition, we found that the hepatic uptake of pDNA involves a specific mechanism similar to, but distinct from, a class A scavenger receptor (SRA), as it was dramatically inhibited by specific polyanions such as polyinosinic acid (poly I) and dextran sulfate but not by polycytidylic acid (poly C) in mice as well as in a rat liver perfusion system; in addition, it was not significantly affected in SRA-knockout mice (3–5). More recently, we suggested that, among the nonparenchymal cells, liver sinusoidal endothelial cells (LSECs), rather than Kupffer cells, made a major contribution to the overall uptake of pDNA, as gadolinium chloride-induced blockade of Kupffer cells did not affect the degree of hepatic uptake of [^{32}P]pDNA in mice (6). However, there has been no direct evidence for the large contribution of LSECs to the hepatic uptake of pDNA.

LSECs are known to play an important role in the induction of immune tolerance (7,8). In addition, the potential capability of LSECs as a major scavenger of circulating DNAs gives rise to the possibility that LSECs participate in the onset of systemic lupus erythematosus, a disease characterized by the production of anti-DNA antibody (9). In order to develop a strategy for optimizing pDNA delivery in gene therapy and DNA vaccination, it is important to elucidate the types of liver cells involved in pDNA uptake because this might be related to pDNA-derived gene expression and pDNA-induced immune responses. In the current study, therefore, we investigated quantitatively the contribution of LSECs to the hepatic uptake of pDNA following intravenous injection in the rat and studied more details of the cellular uptake characteristics of pDNA *in vitro* using primary cultures of rat LSECs.

MATERIALS AND METHODS

Chemicals

[α-^{32}P]dCTP (3000 Ci/mmol) and dextran (MW 70,000) were obtained from Amersham (Buckinghamshire, England). ^{111}Indium chloride was supplied by Nihon Medi-Physics Co. (Takarazuka, Japan). Poly I (MW 103,300) and poly C (MW 99,500) were purchased from Pharmacia (Uppsala, Sweden). Dextran sulfate (MW 150,000) and heparin sodium salt were purchased from Nacalai Tesque (Kyoto, Japan). Type I-A collagenase, dexamethasone, and vascular endothelial growth factor (VEGF) were purchased from Sigma (St. Louis, MO, USA). Type I rat tail collagen and ITS(+) were purchased from BD Biosciences (San Jose, CA, USA). All other chemicals used were of the highest purity available.

Plasmid DNA

pCMV-Luc (10) encoding firefly luciferase was used as a model pDNA throughout the current study. The pDNA amplified in the DH5α strain of *Escherichia coli* was extracted and purified by a QIAGEN Endofree Plasmid Giga Kit (QIAGEN GmvH, Hilden, Germany). The purity was checked by 1% agarose gel electrophoresis followed by ethid-

[1] Department of Biopharmaceutics and Drug Metabolism, Graduate School of Pharmaceutical Sciences, Kyoto University, Kyoto, Japan.
[2] To whom correspondence should be addressed. (e-mail: takakura@pharm.kyoto-u.ac.jp)

ABBREVIATIONS: pDNA, plasmid DNA; poly I, polyinosinic acid; poly C, polycytidylic acid; LSECs, liver sinusoidal endothelial cells; SRA, class A scavenger receptor; TCA, trichloroacetic acid.

0724-8741/04/0700-1223/0 © 2004 Plenum Publishing Corporation

ium bromide staining. The pDNA concentration was measured by UV absorption at 260 nm. For biodistribution or cellular uptake studies, pDNA was radiolabeled with ^{111}In as described below or with [α-^{32}P]dCTP by the nick translation method (11). For confocal microscopic observations, pDNA was labeled with fluorescein using a FastTag FL labeling kit (Vector Laboratories, Burlingame, CA, USA).

Preparation of [^{111}In]pDNA

Radiolabeling of pDNA with ^{111}In was performed by a method described elsewhere (12). Briefly, to a 27.5-μl dimethylsulfoxide solution of 1 mg 4-[*p*-azidosalicylamido]butylamine (ASBA) was added diethylenetriaminepentaacetic acid (DTPA) anhydride (2 mg) under dark-room conditions, and the mixture was incubated at room temperature for 1 h Then, 25 μl pDNA solution (4 mg/ml) was added to the mixture, and the volume was adjusted to 500 μl with phosphate-buffered saline (PBS) of pH 7.4. The mixture was immediately irradiated under a UV lamp (365 nm, UltraViolet Products, Upland, CA, USA) at room temperature for 15 min to obtain DTPA-ASBA coupled pDNA (DTPA-ASBA-pDNA). The product was purified by ethanol precipitation twice and was dissolved in 20 μl acetate buffer (0.1 M, pH 6). To 10 μl sodium acetate solution (1 M) was added 10 μl $^{111}InCl_3$, then 20 μl DTPA-ASBA-pDNA. The mixture was incubated at room temperature for 1 h, and unreacted $^{111}InCl_3$ was removed by ultrafiltration. The purity was checked by Sephadex G-25 column (1 × 40 cm) chromatography and 1% agarose gel electrophoresis.

In Vivo Disposition Studies of pDNA

Male Wistar rats (250 g) were purchased from the Shizuoka Agricultural Co-operate Association for Laboratory Animals (Shizuoka, Japan). All animal experiments were reviewed and approved by the Ethics Committee for Animal Experiments at the Kyoto University.

Rats received [^{32}P]pDNA or [^{111}In]pDNA diluted with unlabeled pDNA (1 mg/kg) in sterilized saline by tail vein injection. The tail vein injection was performed using a 26-gauge needle. Blood was withdrawn from the jugular vein at the indicated times following pDNA injection under anesthesia and then centrifuged to obtain plasma. The rats were euthanized 30 min after urine collection from the urinary bladder, and then the kidney, liver, lung, and heart were excised and rinsed with saline. In the case of [^{32}P]pDNA, the samples of plasma, urine, and small pieces of tissue were dissolved in 0.7 ml Solene-350 at 45°C, followed by the addition of 0.2 ml isopropanol, 0.2 ml H_2O_2, 0.1 ml 5N HCl, and 5 ml Clearsol I (scintillation medium). The radioactivity was measured using a liquid scintillation counter (LSA-500, Beckman, Tokyo, Japan). In the case of [^{111}In]pDNA, the radioactivity of the samples was directly measured in a NaI scintillation counter (ARC-500, Aloka, Tokyo, Japan).

To investigate the intrahepatic distribution of pDNA, rats received [^{111}In]pDNA (1 mg/kg) by tail vein injection under anesthesia. The rats were killed at 30 min, and then the liver was fractionated into parenchymal cells, Kupffer cells, and LSECs as mentioned below. The radioactivity of each cell suspension was measured in a NaI scintillation counter.

Isolation and Culture of Primary LSECs

Isolation of LSECs was performed as previously described (13). Briefly, liver was perfused under anesthesia via the portal vein with Ca^{2+}- and Mg^{2+}-free Hanks' balanced salt solution (HBSS) at 37°C for 10 min at a flow rate of 10–12 ml/min. Then, the liver was perfused with HBSS containing 5 mM Ca^{2+} and 0.05% (w/v) collagenase for 10 min. The digested liver was minced and filtered through a cotton gauze and a nylon mesh (mesh size 45 μm) and then fractionated into hepatocytes and nonparenchymal cells by differential centrifugation. Liver nonparenchymal cells were further separated into LSECs and Kupffer cells by centrifugal elutriation. LSECs were seeded on 24-well plates (1.0×10^6 cells/well), coated beforehand with rat tail collagen, and cultured in RPMI1640 supplemented with 10% fetal calf serum, VEGF (5 μg/ml), ITS(+) (1% v/v), amphotericin B (10 mg/ml), and dexamethasone (0.01 mM) for 4–5 days. The purity of LSECs was checked by immunostaining of factor VIII–related antigen as well as uptake experiment using microparticulates (4.5 μm) and confirmed to be more than 95%. We also ensured the expression of functional receptors on the isolated LSECs in our preliminary *in vitro* uptake experiment using mannosylated BSA (data not shown).

In Vitro Cellular Association Experiments

LSECs were washed three times with 0.5 ml HBSS followed by the addition of 0.5 ml HBSS containing 0.1 μg/ml naked [^{32}P]pDNA. After incubation at 37°C or 4°C for a specified time, incubation medium was removed and the cells were washed five times with ice-cold HBSS and then solubilized with 1.0 ml of 0.3 N NaOH containing 0.1% Triton X-100. Aliquots of the cell lysate were subjected to the determination of ^{32}P radioactivity. To examine the competitive effects of various polyanions on the binding and uptake of pDNA, the described dose of unlabeled pDNA or macromolecules such as poly I, poly C, and dextran sulfate was added to the incubation medium concomitantly with [^{32}P]pDNA.

TCA Precipitation Experiments

To estimate the amount of degradation products of pDNA, following completion of the cellular association experiments, the culture medium and cell lysates were subjected to trichloroacetic acid (TCA) precipitation. After elimination of cellular proteins by extracting with TE buffer-saturated phenol (69% phenol), aliquots of the supernatants and cell lysates were mixed with TCA to give a final concentration of 5% (w/v), kept on ice for 10 min, and then centrifuged at 13,000 rpm for 30 min. The supernatant (TCA-soluble fraction) was subjected to radioactivity measurement. The TCA-soluble fraction is supposed to contain small DNA fragments of degradation products (short oligonucleotides), as longer oligonucleotides (>16-mer) are precipitable in 5% TCA (14).

Confocal Microscopic Study

LSECs cultured on the cover glasses were washed with HBSS and mixed with 5 μg/ml fluorescein-labeled pDNA ([FL]pDNA). After incubation at 37°C or 4°C, the cells were washed and fixed with 4% paraformaldehyde for 1 h. Then, cell sheets were stained with an anti-factor VIII–related an-

tigen mouse IgG (InnoGenex, San Ramon, CA, USA) at 1:200 dilution followed by secondary antibodies, an anti-mouse IgG Alexa Fluor 594 (Molecular Probes, Eugene, OR, USA) at 1:250 dilution. Finally, these samples were subjected to confocal microscopic investigation (MRC-1024, Bio-Rad, Hercules, CA, USA).

RESULTS

In Vivo Disposition of pDNA After Intravenous Injection

First, we examined the *in vivo* disposition of pDNA in rats. Figure 1 shows the time-courses of the plasma concentration of radioactivity and the amounts of radioactivity in the organs and urine at 30 min after intravenous injection of [^{32}P]pDNA or [^{111}In]pDNA (1 mg/kg). pDNA was rapidly eliminated from the circulation and mainly taken up by the liver, similarly to previous studies using mice (3,6). No significant difference was observed, at least during this experimental period, between the radiolabeling methods in terms of the pattern of elimination from plasma and the degree of liver accumulation.

To examine the contribution of liver-constituting cells to the hepatic uptake of pDNA, hepatocytes, LSECs, and Kupffer cells were isolated from the liver following intravenous administration of pDNA. Figure 2 shows the intrahepatic distribution of pDNA at 30 min after intravenous injection of [^{111}In]pDNA at a dose of 1 mg/kg. The amount of pDNA taken up by LSECs and Kupffer cells on a cellular basis (i.e., per 10^8 cells) were significantly greater than that by hepatocytes (Fig. 2A). The relative contributions of hepatocytes, Kupffer cells and LSECs were evaluated on the basis of the numbers of each cell per liver (15,16). As shown in Fig. 2B, pDNA was mostly taken up by LSECs (almost 50% of total hepatic uptake). The estimated total hepatic recovery of injected radioactivity, which was calculated from the data in Fig. 2A on the basis of the number of each cell per 1 g liver assuming the weight of the rat liver to be 8 g, was approximately 70% of the dose, in agreement with the direct measurement of the hepatic accumulation of [^{111}In]pDNA (Fig. 1B). However, in our preliminary study using [^{32}P]pDNA, the estimated liver accumulation following isolation of liver-constituting cells was less than 15% of the dose (data not shown), which was much lower than that determined in Fig. 1B.

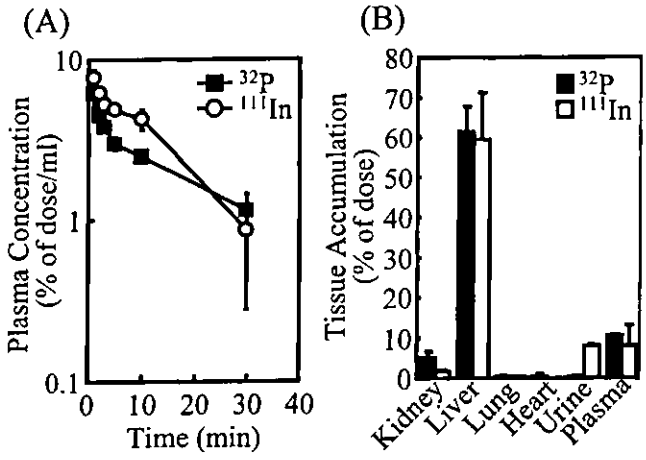

Fig. 1. Time-courses of (A) plasma concentration and (B) tissue accumulation of radioactivity at 30 min after intravenous injection of [^{32}P]pDNA or [^{111}In]pDNA (1 mg/kg) into rats. The results are expressed as mean ± SD (n = 3).

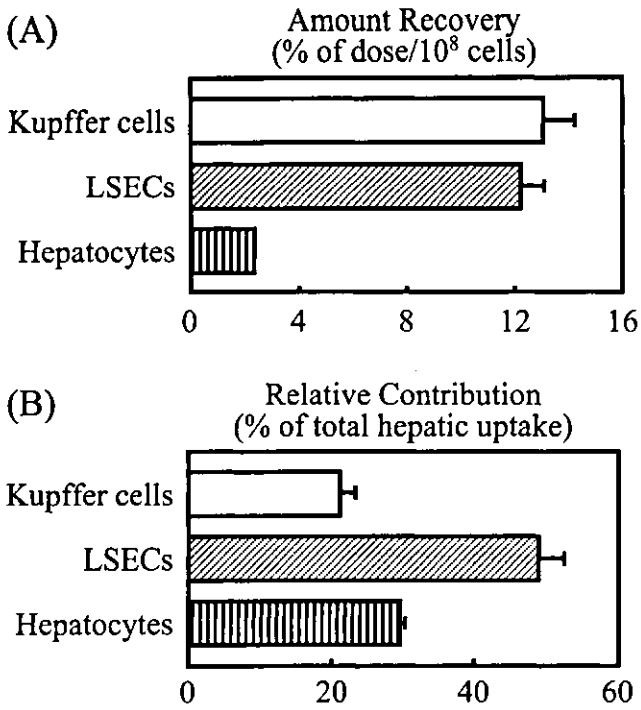

Fig. 2. Intrahepatic distribution of [^{111}In]pDNA (1 mg/kg) on a (A) cellular basis and (B) the relative contribution of each type of liver cell to the total hepatic uptake. Rats were euthanized 30 min after intravenous injection and liver cells were isolated as described in "Materials and Methods." The results are expressed as mean ± SD (n = 3).

Cellular Uptake and Degradation of pDNA in Primary Culture of Rat LSECs

To evaluate the details of the cellular uptake of pDNA by LSECs, *in vitro* studies were performed with primary cultures of rat LSECs. Figure 3 shows the uptake of [FL]pDNA in primary cultures of LSECs assessed by confocal laser scanning microscopy. Fluorescence derived from [FL]pDNA was

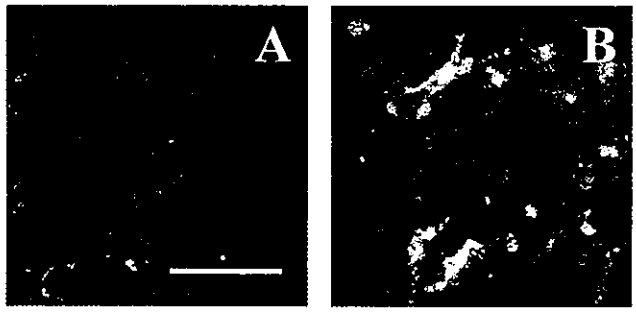

Fig. 3. Confocal microscopic images of LSECs following incubation with [FL]pDNA. The cells were incubated with 0.1 μg/ml [FL]pDNA (green) for 3 h at (A) 4°C or (B) 37°C and fixed with 4% paraformaldehyde and immunostained with anti-factor VIII–related antigen antibody (red). The images shown are typical of those observed in several visual fields. Scale bar represents 50 μm.

restricted to the cell surface or extracellular compartment at 4°C, whereas an intense fluorescence was observed in the intracellular compartment at 37°C.

Figure 4 shows the time-courses of the cellular association and degradation of [^{32}P]pDNA in primary cultures of rat LSECs. The cellular association at 37°C reached a maximum at 1.5 h and then gradually decreased probably due to the release of degradation products into the culture medium. However, at 4°C, a steady increase in the apparent cellular association was observed, although the cells did not appear to internalize pDNA as shown by confocal microscopy. To evaluate the degradation of [^{32}P]pDNA after uptake by LSECs, TCA precipitation experiments were performed. The degradation products of [^{32}P]pDNA in the cellular fraction were at most 2% of the applied dose at 37°C and 4°C (Fig. 4B). On the other hand, a time-dependent dramatic increase was observed in the amount of the degradation products of [^{32}P]pDNA in the culture medium at 37°C, but not at 4°C (Fig. 4C).

Effect of Various Polyanions on Cellular Uptake and Degradation of pDNA in LSECs

We performed competitive studies to examine if the cellular uptake characteristics of pDNA in LSECs were similar to that demonstrated *in vivo* in mice. Figure 5 shows the

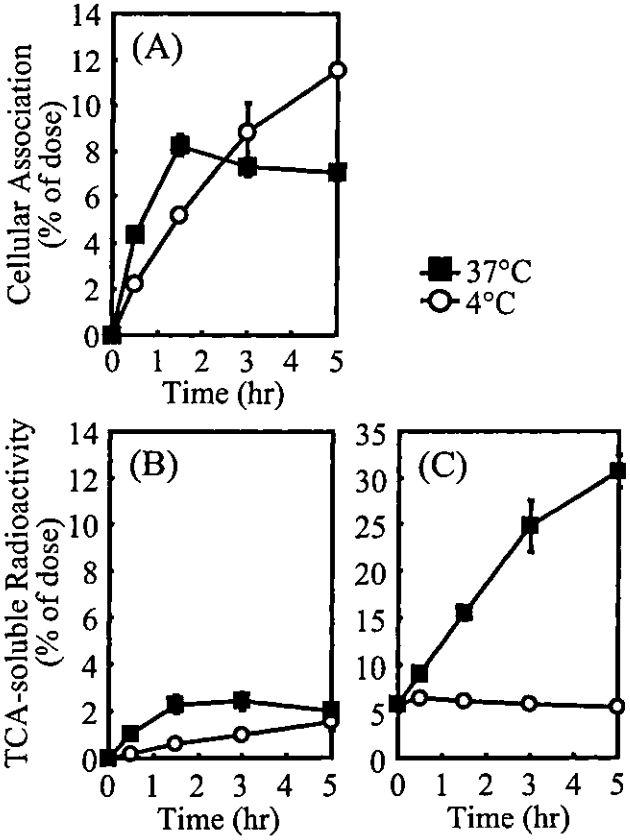

Fig. 4. Time-courses of cellular association of [^{32}P]pDNA with (A) LSECs and TCA-soluble radioactivity in (B) the LSEC cellular fraction and (C) in culture medium. The cells were incubated with [^{32}P]pDNA (0.1 μg/ml) at 37°C (closed square) or 4°C (open circle). Each point represents the mean ± SD (n = 3). The SD was included in the symbol when it was very small.

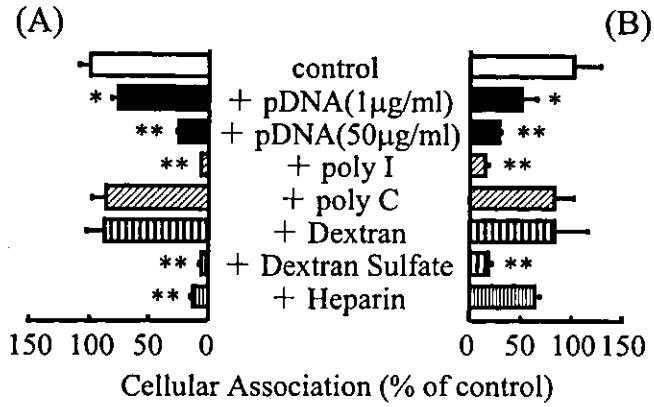

Fig. 5. Competitive effects of various macromolecules on cellular association of [^{32}P]pDNA with LSECs at (A) 4°C or (B) 37°C. The cells were incubated with [^{32}P]pDNA (0.1 μg/ml) for 3 h in the presence or absence of the indicated dose of unlabeled pDNA and various macromolecules (50 μg/ml). The results are expressed as mean ± SD (n = 3). Statistical significance was analyzed by Dunnett's test; $^{**}p < 0.01$, $^{*}p < 0.05$ vs. control.

competitive effects of various macromolecules on the cellular association of [^{32}P]pDNA with LSECs. Excess amounts of unlabeled pDNA inhibited cellular association of [^{32}P]pDNA at 37°C and 4°C. The cellular association was also significantly inhibited by the presence of poly I, dextran sulfate, or heparin, but not by poly C or dextran. To examine further the effect of polyanions on the degradation of [^{32}P]pDNA, the TCA-soluble radioactivity in the culture medium was measured following competitive experiments at 37°C (Fig. 6). Degradation of pDNA was prevented by an excess of unlabeled pDNA and polyanions such as poly I and heparin, which inhibited the cellular association of pDNA.

DISCUSSION

A number of studies involving *in vivo* disposition following intravenous injection of naked DNAs and their complexes, such as single-stranded DNA, double-stranded DNA, oligonucleotide, DNA anti-DNA immune complex, or mononucleosome, have been already reported (17–20). These studies have shown that the liver is the main organ responsible for the rapid clearance of these DNAs from the circulation, while

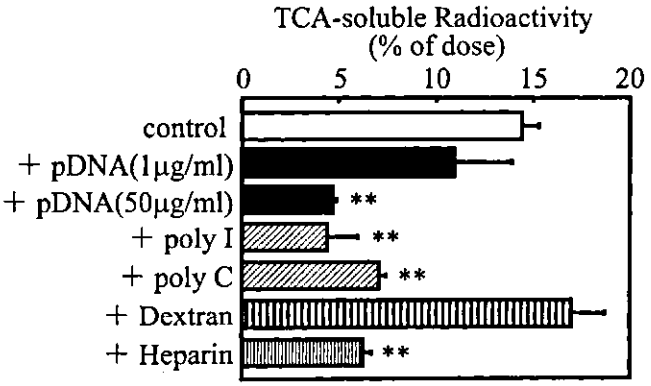

Fig. 6. TCA-soluble radioactivity in the culture medium following competitive experiments at 37°C. The results are expressed as mean ± SD (n = 3). Statistical significance was analyzed by Dunnett's test; $^{**}p < 0.01$ vs. control.

the uptake mechanism and the cell-type(s) contributing to this hepatic uptake remain to be elucidated. We have demonstrated predominant uptake of pDNA by liver nonparenchymal cells (3,4) and suggested the relative importance of LSECs for the overall hepatic uptake of pDNA (6). However, due to lack of direct evidence, more detailed studies need to be performed to confirm the significant contribution of LSECs to pDNA hepatic uptake.

In the current study, we demonstrated efficient uptake and degradation of pDNA by LSECs *in vitro* in primary cell cultures and *in vivo* in rats. We used selective radiolabeling strategies, which allowed us to perform a quantitative analysis of pDNA uptake and degradation. Following intracellular degradation of [^{111}In]pDNA following cellular uptake, ^{111}In should be present as a form of ^{111}In-DTPA-ASBA covalently linked to a single nucleotide or oligonucleotides. Because these metabolites are unlikely to cross biological membranes due to their relatively large size and high hydrophilicity, the ^{111}In-radioactivity could remain within the cells, as is the case of ^{111}In-DTPA-lysine for ^{111}In-labeled protein (21). Therefore, we used [^{111}In]pDNA for the quantitative study of the intrahepatic distribution of pDNA (Fig. 2), expecting a stable retention of the intracellular radioactivity during the isolation steps. Indeed, the intracellular ^{32}P-radioactivity was substantially reduced after the isolation steps (data not shown). However, the amount of degradation product of pDNA could not be determined with [^{111}In]pDNA because [^{111}In]pDNA is unsuitable for the TCA precipitation method. Therefore, [^{32}P]pDNA was used for the *in vitro* experiments involving cellular association and degradation of pDNA (Figs. 4–6) in order to estimate the amount of extracellular or intracellular degradation products by the TCA precipitation method.

We first examined the *in vivo* disposition of pDNA in rats and showed that pDNA was rapidly eliminated from the circulation and taken up by the liver after intravenous injection (Fig. 1), similarly to our previous findings using mice (3,6). A quantitative analysis of the intrahepatic distribution of [^{111}In]pDNA revealed that the amount of radioactivity taken up by LSECs and Kupffer cells, being much higher than those recovered in hepatocytes, was similar in cell number basis, thereby indicating a large contribution of LSECs to the overall hepatic uptake of pDNA following intravenous injection (Fig. 2), as the liver contains 2.5-fold more LSECs than Kupffer cells (15,16). This supports the fact that inhibition of Kupffer cells by gadolinium chloride did not significantly reduce the total hepatic uptake of [^{32}P]pDNA in mice (6). Taken together, the current findings imply a significant role of LSECs in pDNA clearance, in addition to the previous suggestion that the hepatic uptake of intravenously injected pDNA is largely mediated by Kupffer cells (22).

In uptake experiments with primary cultures of LSECs, the degree of the apparent cellular association of [^{32}P]pDNA was similar at 37°C and 4°C (Fig. 4A), although internalization of [FL]pDNA was observed at 37°C but not at 4°C (Fig. 3). The amount of degradation products of [^{32}P]pDNA in the cellular compartment increased rapidly at 37°C, while it was a small fraction of the applied radioactivity, suggesting that rapid degradation of pDNA occurred in LSECs. At the same time, a dramatic increase in the degradation products of [^{32}P]pDNA in the culture medium was observed at 37°C, whereas there was no increase in radioactivity at 4°C (Fig. 4C). These results suggested that pDNA was internalized and rapidly degraded by LSECs and that degraded fragments of pDNA were readily released into the culture medium. The degradation of [^{32}P]pDNA observed in the current study seems to occur predominantly in the intracellular compartment following internalization or on the surface of the LSECs, but not in the culture medium, as no significant degradation was observed during incubation of [^{32}P]pDNA with medium alone, which had been exposed to LSECs for 3 h (data not shown).

A specific mechanism is involved in the cellular uptake process of pDNA by LSECs as shown in the competitive experiment. pDNA uptake and binding were significantly inhibited by excess unlabeled pDNA and some polyanions such as poly I, dextran sulfate, or heparin, but not by others such as poly C or dextran (Fig. 5). This inhibition pattern highly resembles that of our previous *in vivo* study using mice (6), supporting the hypothesis that LSECs make a major contribution to the hepatic uptake of intravenously injected pDNA. Poly I but not poly C is known to form a base quartet-stabilized four strand helix (quadruplex) (23). This hyperstructure would be highly polyanionic. Similar speculation could be applied to polysaccharides such as dextran sulfate and heparin, because they are also highly sulfated. LSECs express various types of receptors essential for endocytosis, such as mannose receptors (24), Fcγ receptors (25), and various classes of scavenger receptors such as SRA, CD36 (class B), LOX-1 (class E), and SREC (class F) (26). Although we could not conclude at this moment which uptake pathway or receptors are involved in pDNA recognition, the results of competitive inhibition experiments have led to the hypothesis that putative receptor(s) on LSECs might recognize pDNA based on its highly polyanionic nature. We have demonstrated that pDNA is taken up by cultured macrophages (27), dendritic cells (28), and brain microvessel endothelial cells (29) via a specific mechanism resembling scavenger receptors. In addition, class A scavenger receptors (SRA) that recognize a wide variety of anionic macromolecules are unlikely to be responsible for pDNA uptake as shown by *in vivo* and *in vitro* experiments using SRA-knockout mice and peritoneal macrophages from these animals (5). Because the inhibition pattern of pDNA uptake is very similar in those different cell types, the cellular uptake mechanisms might be highly conserved among cells including LSECs. It might not be excluded for *in vivo* situation that the serum cationic proteins or complement proteins interact with circulating pDNA and this could facilitate the recognition and uptake of pDNA by LSECs. However, in our previous study using rat liver perfusion system, pDNA was taken up by the liver nonparenchymal cells in the absence of serum via a similar mechanisms involved *in vivo* following intravenous injection. Because serum-free HBSS was used in the current *in vitro* study to avoid serum nuclease-mediated pDNA degradation before recognition by LSECs, the observed pDNA uptake by LSECs was not dependent on these serum proteins. Though further studies are required to elucidate the mechanism involved in pDNA uptake by LSECs, the high density of negative charges arising from the phosphate groups of pDNA may be an important factor.

It is also suggested that pDNA taken up by LSECs is susceptible to degradation. It is likely that the degradation occurs enzymatically predominantly inside the cells probably by DNase II in lysosomes (30) following internalization via

endocytosis, although degradation on the surface of the cells by membrane-bound DNase is not excluded (22). In fact, the degradation was strongly inhibited by cellular uptake inhibitors (Fig. 6), suggesting that the uptake of pDNA by LSECs via the specific mechanism seems to be indispensable for pDNA degradation. This implies that the specific uptake is associated with the pDNA degradation in the LSECs. Unexpectedly, the degradation of pDNA appeared to be inhibited by poly C. Although poly C showed no inhibitory effect on pDNA uptake and binding (Fig. 5), it might affect pDNA degradation in a nonspecific manner.

In conclusion, the current study has shown that LSECs, as well as Kupffer cells, play a key role in the clearance of circulating pDNA following intravenous injection, providing a larger contribution to the overall hepatic uptake of pDNA. We have demonstrated that naked pDNA is efficiently taken up via a specific mechanism and rapidly degraded by LSECs, the degradation products being released into the extracellular space. These findings provide useful information for pDNA delivery in gene therapy and DNA vaccination procedures.

ACKNOWLEDGMENTS

This work was supported, in part, by a grant-in-aid for Scientific Research from the Ministry of Education, Culture, Sports, Science and Technology, Japan.

REFERENCES

1. M. Nishikawa and L. Huang. Nonviral vectors in the new millennium: delivery barriers in gene transfer. *Hum. Gene Ther.* **12**:861–870 (2001).
2. N. Kobayashi, M. Nishikawa, and Y. Takakura. Gene therapy and gene delivery. In B. Wang, T. Siahaan, and R. Soltero (eds.), *Delivery Issues in Drug Discovery*, in press.
3. K. Kawabata, Y. Takakura, and M. Hashida. The fate of plasmid DNA after intravenous injection in mice: involvement of scavenger receptors in its hepatic uptake. *Pharm. Res.* **12**:825–830 (1995).
4. M. Yoshida, R. I. Mahato, K. Kawabata, Y. Takakura, and M. Hashida. Disposition characteristics of plasmid DNA in the single-pass rat liver perfusion system. *Pharm. Res.* **13**:599–603 (1996).
5. Y. Takakura, T. Takagi, M. Hashiguchi, M. Nishikawa, F. Yamashita, T. Doi, T. Imanishi, H. Suzuki, T. Kodama, and M. Hashida. Characterization of plasmid DNA binding and uptake by peritoneal macrophages from class A scavenger receptor knockout mice. *Pharm. Res.* **16**:503–508 (1999).
6. N. Kobayashi, T. Kuramoto, K. Yamaoka, M. Hashida, and Y. Takakura. Hepatic uptake and gene expression mechanisms following intravenous administration of plasmid DNA by conventional and hydrodynamics-based procedures. *J. Pharmacol. Exp. Ther.* **297**:853–860 (2001).
7. P. A. Knolle and G. Gerken. Local control of the immune response in the liver. *Immunol. Rev.* **174**:21–34 (2000).
8. A. Limmer, J. Ohl, C. Kurts, H. G. Ljunggren, Y. Reiss, M. Groettrup, F. Momburg, B. Arnold, and P. A. Knolle. Efficient presentation of exogenous antigen by liver endothelial cells to CD8+ T cells results in antigen-specific T-cell tolerance. *Nat. Med.* **6**:1348–1354 (2000).
9. D. S. Pisetsky. Anti-DNA and autoantibodies. *Curr. Opin. Rheumatol.* **12**:364–368 (2000).
10. T. Nomura, K. Yasuda, T. Yamada, S. Okamoto, R. I. Mahato, Y. Watanabe, Y. Takakura, and M. Hashida. Gene expression and antitumor effects following direct interferon (IFN)-gamma gene transfer with naked plasmid DNA and DC-chol liposome complexes in mice. *Gene Ther.* **6**:121–129 (1999).
11. J. Sambrook, E. F. Fritsch, and T. Maniatis. *Molecular Cloning*, Cold Spring Harbor Laboratory, Cold Spring Harbor, New York, 1989.
12. M. Nishikawa, T. Nakano, T. Okabe, N. Hamaguchi, Y. Yamasaki, Y. Takakura, F. Yamashita, and M. Hashida. Residualizing indium-111-radiolabel for plasmid DNA and its application to tissue distribution study. *Bioconjug. Chem.* **14**:955–961 (2003).
13. J. F. Nagelkerke, K. P. Barto, and T. J. van Berkel. In vivo and in vitro uptake and degradation of acetylated low density lipoprotein by rat liver endothelial, Kupffer, and parenchymal cells. *J. Biol. Chem.* **258**:12221–12227 (1983).
14. J. E. Cleaver and H. W. Boyer. Solubility and dialysis limits of DNA oligonucleotides. *Biochim. Biophys. Acta* **262**:116–124 (1972).
15. R. Blomhoff, H. K. Blomhoff, H. Tolleshaug, T. B. Christensen, and T. Berg. Uptake and degradation of bovine testes beta-galactosidase by parenchymal and nonparenchymal rat liver cells. *Int. J. Biochem.* **17**:1321–1328 (1985).
16. S. Magnusson and T. Berg. Endocytosis of ricin by rat liver cells in vivo and in vitro is mainly mediated by mannose receptors on sinusoidal endothelial cells. *Biochem. J.* **291**:749–755 (1993).
17. W. Emlen and M. Mannik. Effect of DNA size and strandedness on the in vivo clearance and organ localization of DNA. *Clin. Exp. Immunol.* **56**:185–192 (1984).
18. W. Emlen and G. Burdick. Clearance and organ localization of small DNA anti-DNA immune complexes in mice. *J. Immunol.* **140**:1816–1822 (1988).
19. V. J. Gauthier, L. N. Tyler, and M. Mannik. Blood clearance kinetics and liver uptake of mononucleosomes in mice. *J. Immunol.* **156**:1151–1156 (1996).
20. W. Emlen and M. Mannik. Kinetics and mechanisms for removal of circulating single-stranded DNA in mice. *J. Exp. Med.* **147**: 684–699 (1978).
21. F. N. Franano, W. B. Edwards, M. J. Welch, and J. R. Duncan. Metabolism of receptor targeted 111In-DTPA-glycoproteins: identification of 111In-DTPA-epsilon-lysine as the primary metabolic and excretory product. *Nucl. Med. Biol.* **21**:1023–1034 (1994).
22. W. Emlen, A. Rifai, D. Magilavy, and M. Mannik. Hepatic binding of DNA is mediated by a receptor on nonparenchymal cells. *Am. J. Pathol.* **133**:54–60 (1988).
23. A. M. Pearson, A. Rich, and M. Krieger. Polynucleotide binding to macrophage scavenger receptors depends on the formation of base-quartet-stabilized four-stranded helices. *J. Biol. Chem.* **268**: 3546–3554 (1993).
24. A. L. Hubbard, G. Wilson, G. Ashwell, and H. Stukenbrok. An electron microscope autoradiographic study of the carbohydrate recognition systems in rat liver. I. Distribution of 125I-ligands among the liver cell types. *J. Cell Biol.* **83**:47–64 (1979).
25. H. Muro, H. Shirasawa, M. Maeda, and S. Nakamura. Fc receptors of liver sinusoidal endothelium in normal rats and humans. A histologic study with soluble immune complexes. *Gastroenterology* **93**:1078–1085 (1987).
26. V. Terpstra, E. S. van Amersfoort, A. G. van Velzen, J. Kuiper, and T. J. van Berkel. Hepatic and extrahepatic scavenger receptors: function in relation to disease. *Arterioscler. Thromb. Vasc. Biol.* **20**:1860–1872 (2000).
27. T. Takagi, M. Hashiguchi, R. I. Mahato, H. Tokuda, Y. Takakura, and M. Hashida. Involvement of specific mechanism in plasmid DNA uptake by mouse peritoneal macrophages. *Biochem. Biophys. Res. Commun.* **245**:729–733 (1998).
28. T. Yoshinaga, K. Yasuda, Y. Ogawa, and Y. Takakura. Efficient uptake and rapid degradation of plasmid DNA by murine dendritic cells via a specific mechanism. *Biochem. Biophys. Res. Commun.* **299**:389–394 (2002).
29. M. Nakamura, P. Davila-Zavala, H. Tokuda, Y. Takakura, and M. Hashida. Uptake and gene expression of naked plasmid DNA in cultured brain microvessel endothelial cells. *Biochem. Biophys. Res. Commun.* **245**:235–239 (1998).
30. C. Odaka and T. Mizuochi. Role of macrophage lysosomal enzymes in the degradation of nucleosomes of apoptotic cells. *J. Immunol.* **163**:5346–5352 (1999).

0022-3565/04/3082-688–693$20.00
THE JOURNAL OF PHARMACOLOGY AND EXPERIMENTAL THERAPEUTICS

JPET 308:688–693, 2004

Vol. 308, No. 2
59931/1126476
Printed in U.S.A.

Vector-Based in Vivo RNA Interference: Dose- and Time-Dependent Suppression of Transgene Expression

Naoki Kobayashi, Yumi Matsui, Atsushi Kawase, Kazuhiro Hirata, Makoto Miyagishi,[1] Kazunari Taira,[1] Makiya Nishikawa, and Yoshinobu Takakura

Department of Biopharmaceutics and Drug Metabolism, Graduate School of Pharmaceutical Sciences, Kyoto University, Sakyo-ku, Kyoto, Japan (N.K., Y.M., A.K., M.N., Y.T.); Department of Chemistry and Biotechnology, School of Engineering, the University of Tokyo, Hongo, Tokyo, Japan (M.M., K.T.); and Gene Discovery Research Center, National Institute of Advanced Industrial Science and Technology (AIST), Ibaraki Japan (M.M., K.T.)

Received September 12, 2003; accepted November 7, 2003

ABSTRACT

RNA interference (RNAi) induced by delivery of a small-interfering RNA (siRNA)-expressing vector was characterized in mice. siRNA-expressing plasmid DNA (pDNA) was injected by a hydrodynamics-based procedure along with pDNA encoding an exogenous target luciferase gene. A comparative study showed that stem-loop-type siRNA-expressing pDNA was superior, in terms of the transgene suppressive efficacy, to the tandem-type in the liver following systemic delivery of these pDNAs. Transgene suppression occurred in the liver, kidney, and lung as well as muscle. The degree of suppression was dependent on the dose of siRNA-expressing pDNA and the time at which transgene expression was determined following simultaneous injection of siRNA-expressing and target pDNAs. A reduction in transgene expression became apparent at 1 day after injection, whereas a lower degree of inhibition was obtained before this, as early as 6 h even in mice treated with an excess of siRNA-expressing pDNA. These results suggest that delivery of siRNA-expressing pDNA requires a period of time for induction of RNAi. A study of sequential injections revealed that prior injection of siRNA-expressing pDNA produced a significant suppression for at least 1 day, which disappeared within 4 days. Confocal microscopic studies indicated that the localization of the cells with successful delivery of transgene was different between primary and secondary hydrodynamics-based injections, accounting for the less effective inhibition following the sequential injections. Taken together, these results demonstrate that vector-based in vivo RNAi is a dose- and time-dependent process and offers the possibility of suppressing endogenous targets in a variety of somatic cells.

RNA interference (RNAi) is known as a powerful tool for post-transcriptional gene silencing and expected to be involved in gene therapy strategies (Hannon, 2002; Hutvagner and Zamore, 2002; Dykxhoorn et al., 2003). Small-interfering RNA (siRNA), generated via cleavages of long double-stranded RNA by a member of the RNase III family, Dicer, and typically consisting of two 21- to 23-nucleotide single-stranded RNAs that form a duplex with 2- to 4-nucleotide 3′ overhangs, plays a pivotal role in the RNAi process. Application of RNAi to mammals remained limited due to a sequence-nonspecific gene suppression via the interferon response triggered by long (>30 nucleotides) double-stranded RNA, until it was shown that the use of synthetic siRNA could induce RNAi in mammalian cells without nonspecific inhibition (Caplen et al., 2001; Elbashir et al., 2001). Immediately after the reports of successful induction of RNAi in mammalian cells, we and other groups (Brummelkamp et al., 2002; Lee et al., 2002; Miyagishi and Taira, 2002; Paddison et al., 2002a; Paul et al., 2002; Sui et al., 2002; Yu et al., 2002; Kawasaki and Taira, 2003) developed a vector-based siRNA expression system driven by Pol III promoter such as U6, H1, or transfer RNA^{val} promoter and demonstrated effective induction of vector-based RNAi. Although synthetic siRNA is a functional molecule by itself, which can be incorporated into the RNA-induced silencing complex (RISC) and can guide RISC to the target mRNA of a complementary sequence, direct application of siRNA is accompanied by several disadvantages including an immediate disappearance of the knockdown effect due to the lack of siRNA amplification mechanisms in mammalian cells (Chiu and Rana, 2002; Zamore, 2002; Zeng and Cullen, 2002; Stein et al., 2003),

This work was supported in part by a grant-in-aid for Scientific Research from the Ministry of Education, Culture, Sports, Science and Technology, Japan.
Article, publication date, and citation information can be found at http://jpet.aspetjournals.org.
DOI: 10.1124/jpet.103.059931.

ABBREVIATIONS: RNAi, RNA interference; siRNA, small-interfering RNA; pDNA, plasmid DNA; RISC, RNA-induced silencing complex; GFP, green fluorescent protein; EGFP, enhanced GFP; DsRed, red fluorescent protein.

difficulty in regulating its activities, and the inconvenience and high expense associated with its use. On the contrary, siRNA-expressing vector, which works as a platform to produce a large amount of siRNA for a relatively longer period, can potentially circumvent these problems and is a versatile method of application of RNAi.

For gene function research in animals, RNAi-induced knockdown of genes of interest is attractive for its speed, usefulness, and lower cost, compared with the time-consuming conventional strategies such as gene targeting by homologous recombination. Moreover, introduction of siRNA allows us to achieve simultaneous knockdown of multiple genes or transient knockdown of lethal genes that would otherwise prevent us from investigating their functions in postnatal animals. Therefore, in vivo application of RNAi is likely to prove very popular in terms of functional analysis of unknown genes in addition to therapeutic applications to treat viral infections or tumors. Recently, Song et al. (2003) demonstrated that frequent hydrodynamics-based injections of synthetic siRNA dramatically reduced mRNA and protein levels of the targeted gene-encoding Fas receptor and protected mice from liver failure and fibrosis in experimental hepatitis. Local administrations of synthetic siRNA have been shown to suppress endogenous target genes for agouti-related peptide in the brain (Makimura et al., 2002) and for vascular endothelial growth factor in the eyes (Reich et al., 2003). Intraperitoneal delivery of siRNA/lipid-based transfection reagent complexes resulted in suppression of endogenous β-catenin gene expression in grafted colon cancer cells (Verma et al., 2003) and inhibition of lipopolysaccharide-induced TNF-α gene overexpression (Sorensen et al., 2003). Successful results involving in vivo gene silencing of endogenous targets were achieved predominantly by use of synthetic siRNA. On the other hand, in vivo gene silencing with siRNA-expressing vector has been restricted to topical application (Makimura et al., 2002) or targeting transgenes such as luciferase gene (Lewis et al., 2002; McCaffrey et al., 2002a) and hepatitis B virus mRNA (McCaffrey et al., 2003), apart from a reduction in the endogenous β-glucuronidase mRNA level by adenovirus vector-mediated siRNA delivery (Xia et al., 2002). The delayed success of nonviral vector-based approaches might be attributed in part to the lack of information about vector-based in vivo RNAi. Therefore, in the present study, we characterized the suppression of transgene expression by vector-based RNAi in adult mice, using siRNA-expressing plasmid DNA driven by human U6 promoter.

Materials and Methods

Plasmid DNA (pDNA). siRNA-expressing pDNAs driven by human U6 promoter were constructed from piGENE hU6 vector (iGENE Therapeutics, Tsukuba, Japan) according to the instructions (Miyagishi and Taira, 2003). pU6-stem21 transcribes a single-stranded RNA 5′-GUG CGU UGU UGG UGU UAA UCC UUC AAG AGA GGG UUG GCA CCA GCA GCG CAC UUU U-3′, which forms stem-loop-structured siRNA, targeted to pGL3 firefly luciferase$^+$ mRNA (targeted sequence: GTG CGC TGC TGG TGC CAA CCC), with loop sequences of UUCAAGAGA (Brummelkamp et al., 2002). pU6-tandem19 or pU6-tandem26 transcribe 19- or 26-mer, respectively, of both sense and antisense RNAs that form siRNA with a four nucleotide overhang at each 3′ end, targeted to pGL3 firefly luciferase$^+$ mRNA (targeted sequence: GTG CGC TGC TGG TGC CAA C for tandem19 and GTG CGC TGC TGG TGC CAA CCC TAT TC for tandem26). pU6-tandem(GL2)19 produces the same siRNA as pU6-tandem19 except that pGL2 firefly luciferase mRNA is targeted instead of pGL3 luciferase$^+$ (targeted sequence: GTG CGT TGC TAG TAC CAA C). piGENE hU6 vector, which transcribes nonrelated sequences of RNA 5′-GUG AGC AGG UGU AAA GCC ACC AUG GAA GAC ACC UGC CAA CUU UU-3′ with partial duplex formation, was used as a control pDNA throughout the present study. pGL3-control (Promega, Madison, WI) was used as target firefly *Photinus pyralis* luciferase$^+$-expressing pDNA. pRL-SV40 (Promega) encoding sea pansy *Renilla reniformis* luciferase was used as an internal control. pEGFP-N1 encoding enhanced green fluorescent protein (EGFP), pEGFP-F encoding farnesylated EGFP, a modified form of EGFP to bind to the plasma membrane, and pDsRed2-N1 encoding red fluorescent protein DsRed2 were purchased from BD Biosciences Clontech (Palo Alto, CA). We used pEGFP-F for the primary hydrodynamics-based injection to avoid an effusion of the transgene product by the secondary hydrodynamics-based injection, since the unmodified EGFP might diffuse into the circulation following a large-volume injection (Kobayashi et al., 2004). Each pDNA was amplified in the DH5α strain of *Escherichia coli* and purified using a QIAGEN Endofree Plasmid Giga kit (QIAGEN GmbH, Hilden, Germany) or a Geno Pure Plasmid Maxi kit (Roche Diagnostics Corporation, Indianapolis, IN). The purity was checked by agarose gel electrophoresis followed by ethidium bromide staining.

Mice and Intravenous Injection. Four-week-old female ddY mice (approximately 20 g body weight), purchased from Shizuoka Agricultural Cooperative Association for Laboratory Animals (Shizuoka, Japan), were used for all experiments. All animal experiments were brought under deliberation and approved for the Ethics Committee for Animal Experiments at the Kyoto University. Mice received an intravenous injection or an intramuscular injection of pDNAs. The intravenous injection was performed by the hydrodynamics-based procedure (Liu et al., 1999) where the described amount of pDNAs dissolved in 1.6 ml of saline (unless otherwise mentioned) were injected into the tail vein over less than 5 s using a 26-gauge needle.

Luciferase Assay. To determine luciferase activities, mice underwent euthanasia at the indicated time and the organs including the liver, kidney, lung, and muscle were excised and homogenized in 5 ml/g (liver and muscle) or 4 ml/g (kidney and lung) lysis buffer (0.1 M Tris, 0.05% Triton X-100, 2 mM EDTA, pH 7.8). The homogenate was subjected to three cycles of freezing (−190°C) and thawing (37°C) and centrifuged at 13,000*g* for 10 min at 4°C. Then, appropriately diluted supernatant was mixed with luciferase assay buffer (PicageneDual, Toyo Ink, Tokyo, Japan), and the chemiluminescence produced was measured in a luminometer (Lumat LB 9507; EG and G Berthold, Bad Wildbad, Germany). Following subtraction of the background activity for the liver homogenate without injection, the ratio of the activity of firefly luciferase$^+$ (*Pp*-Luc$^+$) to sea pansy luciferase (*Rr*-Luc) was calculated to correct for differences in transfection efficiency among mice. The ratios were normalized to give percent values relative to those of the corresponding control mice. We set the dose of pGL3-control and pRL-SV40 for the raw values of the luciferase activities to be always at least 10-fold higher than those of the background derived from the liver homogenate of mice without injection.

Confocal Microscopic Study of Liver Sections. Mice were euthanized by cutting the vena cava, and the liver was gently infused with 2 ml of saline through the portal vein to remove the remaining blood. The liver was then embedded in Tissue-Tek OCT embedding compound (Sakura Finetechnical Co., Ltd., Tokyo, Japan), frozen in liquid nitrogen, and stored in 2-methyl butanol at −80°C. Frozen liver sections (8-μm thick) were made using a cryostat (Jung Frigocut 2800E; Leica Microsystems AG, Wetzlar, Germany) by the routine procedure. The sections were directly subjected to confocal microscopy (MRC-1024; Bio-Rad, Hercules, CA) without any fixation, since the fixation step caused massive loss of GFP or DsRed due to

immediate dissolution in the fixation buffer in our preliminary experiments.

Results

Interfering Efficiency of Stem-Loop-Type and Tandem-Type siRNA-Expressing Vectors in Vivo. To determine the preference in the RNAi-inducing efficiency of tandem-type and stem-loop-type siRNA-expressing pDNA in vivo, we first compared the suppressive effect in the liver following simultaneous injection of either type of siRNA-expressing pDNA and target and internal control luciferase-expressing pDNAs by the hydrodynamics-based procedure. As shown in Fig. 1, transgene expression of targeted firefly luciferase$^+$ (*Pp*-Luc$^+$) was significantly inhibited in mice treated with pU6-tandem26 or pU6-stem21, but not with pU6-tandem(GL2)19, in agreement with the results of in vitro cell culture (data not shown). It was also revealed that pU6-tandem26, which expresses a longer RNA duplex of 26 nucleotides, was superior in inhibitory activity to the pU6-tandem19, which expresses a 19-nucleotide RNA duplex under these experimental conditions (Fig. 1). Since pU6-stem21, which generates the shorter 21-nucleotide RNA duplex, appeared more effective than tandem-type siRNA-expressing pDNAs, we used pU6-stem21 as a model siRNA-expressing vector throughout the following studies.

Vector-Based RNAi in a Variety of Tissues Following Simultaneous Injection of siRNA-Expressing and Target pDNAs. We examined whether transgene suppression was obtained in vivo in a variety of tissues by systemic or local delivery of siRNA-expressing pDNA. Figure 2 shows the inhibitory effect of siRNA-expressing pDNA on transgene expression of the exogenous firefly luciferase gene. In this set of experiments, we used a higher amount of each pDNA to obtain enough luciferase activities for an accurate analysis in the kidney or lung, based on the fact that the level of transgene expression in these organs is approximately 5 to 6 orders of magnitude lower than that in the liver following the hydrodynamics-based procedure (Liu et al., 1999; Kobayashi et al., 2002). As a result, a marked reduction of transgene expression was observed in various organs, predominantly in the liver, following intravenous injection of the pDNAs (Fig. 2). RNAi-induced transgene suppression also occurred in the muscle following intramuscular injections (Fig. 2).

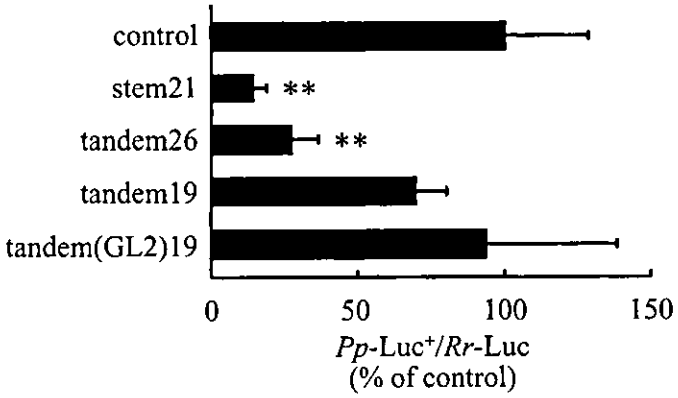

Fig. 1. Comparison of interfering efficiency of various siRNA-expressing pDNAs in the liver. Mice received an intravenous injection of different forms of siRNA-expressing pDNA (10 μg) along with pGL3-control (3 μg) and pRL-SV40 (3 μg) by the hydrodynamics-based procedure. Luciferase activities in the liver were determined 3 days after injection. The results are expressed as the mean ± S.D. ($n > 4$). Statistic significance was analyzed by Dunnett's test; **, $P < 0.01$ versus control.

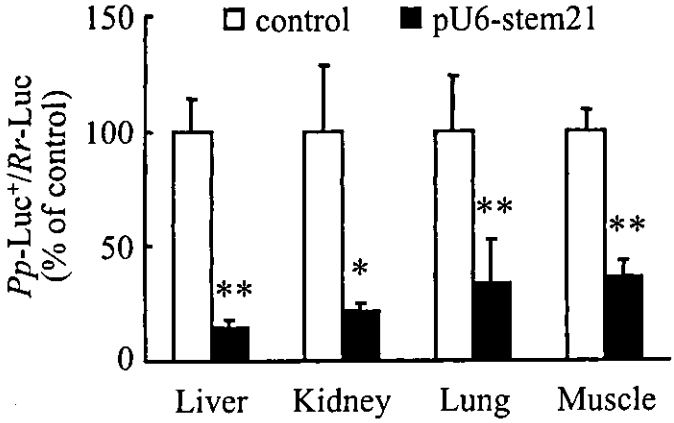

Fig. 2. RNA interference in various organs following siRNA-expressing pDNA injection. Mice received an intravenous injection of piGENE hU6 or pU6-stem21 (80 μg), pGL3-control (10 μg), and pRL-SV40 (10 μg) by the hydrodynamics-based procedure, or an intramuscular injection of piGENE hU6 or pU6-stem21 (20 μg), pGL3-control (1 μg), and pRL-SV40 (1 μg) in a volume of 50 μl. Luciferase activities in the liver, kidney, and lung or treated muscle were determined 1 day after intravenous injection or 3 days after intramuscular injection, respectively. The results are expressed as the mean ± S.D. ($n = 4$). Significantly different from the corresponding control: *, $P < 0.05$; **, $P < 0.01$.

Dose- and Time-Dependent Transgene Suppression in Vector-Based in Vivo RNAi. To examine any dose dependence in the suppressive effect in vector-based RNAi, we injected into mice increasing amounts of effector pDNA (pU6-stem21) and a fixed amount of target pDNAs (pGL3-control and pRL-SV40) and determined the degree of transgene suppression after 3 days. As shown in Fig. 3, inhibitory effect was clearly correlated with the dose of effector pDNA injected, with 97% inhibition in mice treated with 100 μg of pU6-stem21. We further investigated the transgene suppression of siRNA-expressing pDNA at different times after simultaneous injection of effector and target pDNAs. A marked

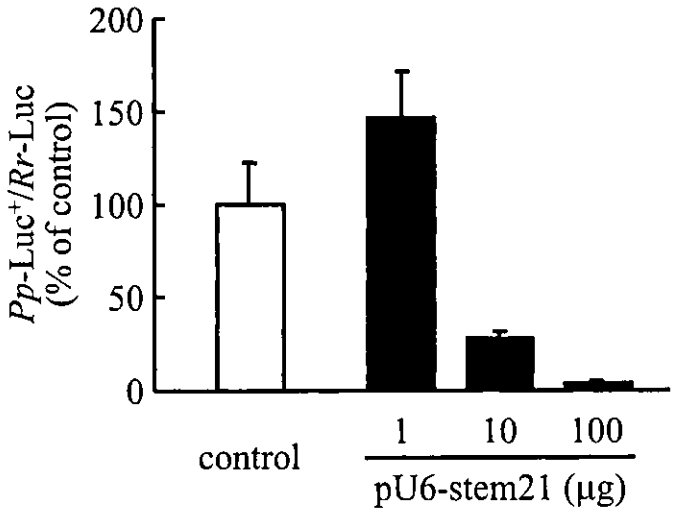

Fig. 3. Effect of dose on the interfering efficiency of siRNA-expressing pDNA in the liver. Mice received an intravenous injection of the indicated dose of pU6-stem21, pGL3-control (3 μg), and pRL-SV40 (3 μg) by the hydrodynamics-based procedure. Control mice were injected with piGENE hU6 (100 μg), pGL3-control (3 μg), and pRL-SV40 (3 μg). Luciferase activities in the liver were determined 3 days after injection. The results are expressed as the mean ± S.D. ($n > 3$).

suppression (more than 90%) of transgene expression was obtained from day 1 to day 11 after injection (Fig. 4). However, in the earlier period, only a weak inhibitory effect was seen at 6 h after injection. To examine whether a suppressive effect becomes apparent even at the earlier period following a reduction in the relative amount of target mRNA, we injected into mice a fixed amount of effector pDNA and decreasing amounts of target pDNAs and determined the luciferase activities as early as 6 h after injection. As a result, a dose-dependent decrease in the *Pp*-Luc$^+$/*Rr*-Luc value was observed, whereas the suppression was limited to 50% inhibition at most in mice injected with 0.001 μg of target pDNA (Fig. 5).

Duration of Interfering Activity Following Hydrodynamics-Based Delivery of siRNA-Expressing Vector. To estimate the duration of suppressing effect of siRNA-expressing pDNA injection, we performed a study of sequential hydrodynamics-based injections of siRNA-expressing pU6-stem21 followed by target pGL3-control and internal control pRL-SV40 at various time intervals. Figure 6 shows the inhibitory effect of siRNA-expressing pDNA injected at various time points before the target pDNA, and in each case, transgene expression was determined at 6 h after the target pDNA injection. The *Pp*-Luc$^+$/*Rr*-Luc values were reduced in mice following injection of pU6-stem21 6 h or 1 day before, but not in mice following 4- or 11-day prior injection (Fig. 6).

Difference in Localization of Transgene-Expressing Cells Following Simultaneous or Sequential Hydrodynamics-Based Delivery of pDNAs. To examine the intrahepatic localization of the transgene-expressing cells following the hydrodynamics-based procedure, we injected mice with GFP-expressing pDNA and/or DsRed-expressing pDNA. Figure 7 shows the results of confocal microscopic observation of the liver sections. A simultaneous delivery of pEGFP-N1 and pDsRed2-N1 resulted in almost complete overlap of the green and the red signals in the identical cells (Fig. 7A), whereas both GFP and DsRed double-positive cells were very rare following the sequential delivery of pEGFP-F and pDsRed2-N1 (Fig. 7B).

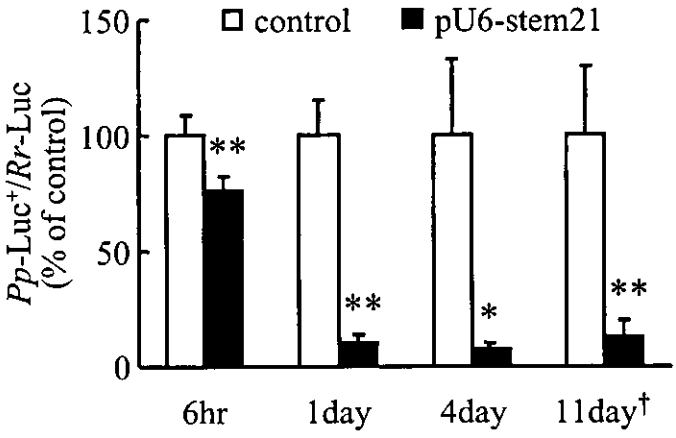

Fig. 4. RNA interference at different times in the liver following simultaneous injection of siRNA-expressing pDNA and target pDNA. Mice received an intravenous injection of piGENE hU6 or pU6-stem21 (10 μg), pGL3-control (3 μg), and pRL-SV40 (3 μg) by the hydrodynamics-based procedure. Luciferase activities in the liver were determined at the indicated times after injection. †, the data for day 11 was calculated without correction by the internal control due to the *Rr*-Luc activity being of the same order of magnitude as the liver background. The results are expressed as the mean ± S.D. (n = 4). **, $P < 0.01$.

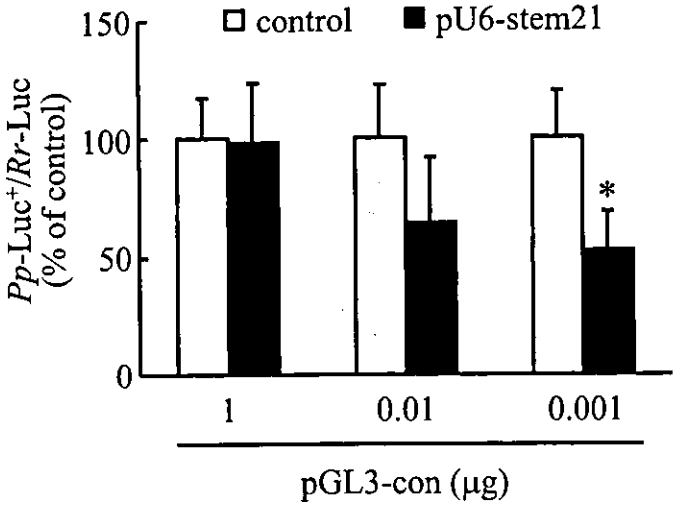

Fig. 5. Effect of target amount on the interfering efficiency of siRNA-expressing pDNA in the liver at an earlier phase. Mice received an intravenous injection of piGENE hU6 or pU6-stem21 (10 μg), pGL3-control, and pRL-SV40 (1 and 1 μg, 0.01 and 0.01 μg, or 0.001 and 0.01 μg, respectively) by the hydrodynamics-based procedure. Luciferase activities in the liver were determined 6 h after injection. The results are expressed as the mean ± S.D. ($n > 3$). *, $P < 0.05$.

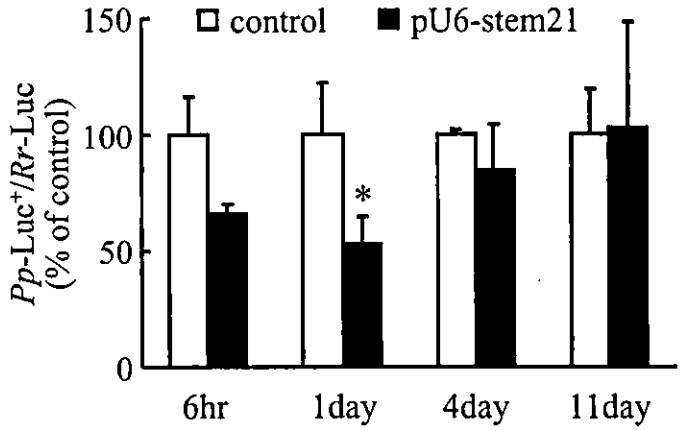

Fig. 6. Effect of time intervals on RNA interference in the liver following sequential injections of siRNA-expressing pDNA and target pDNA. Mice received an intravenous injection of piGENE hU6 or pU6-stem21 (10 μg) by the hydrodynamics-based procedure. Then, at the indicated times, mice were injected again with target pDNAs, pGL3-control (0.01 μg) and pRL-SV40 (0.1 μg), by the hydrodynamics-based procedure in a volume of 1.6 ml (6 h and 1 day), 2.7 ml (4 days), or 3.2 ml (11 days). Luciferase activities in the liver were determined 6 h after injection of target pDNAs. The results are expressed as the mean ± S.D. ($n > 3$). *, $P < 0.05$.

Discussion

The efficiency of gene silencing in vector-based RNAi depends on the characteristics of the siRNA-expressing system, in addition to various factors involved in the siRNA itself. Various types of vectors have been designed to generate siRNA (Tavernarakis et al., 2000; Svoboda et al., 2001; Brummelkamp et al., 2002; Lee et al., 2002; McManus et al., 2002; Miyagishi and Taira, 2002; Paddison et al., 2002a,b; Paul et al., 2002; Sui et al., 2002; Yu et al., 2002; Kawasaki and Taira, 2003), and these siRNA-expression systems can be basically divided into two approaches: the sense and the antisense strands of siRNA are expressed from different cassettes aligned in tandem in the same construct (i.e., tandem-type), or the sense and the antisense strands are expressed as a connected RNA with several intermediate bases of in-

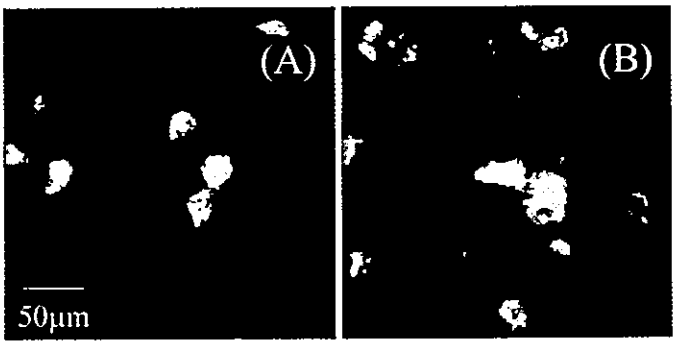

Fig. 7. Confocal microscopic images of the liver following intravenous injection of GFP-expressing pDNA and DsRed-expressing pDNA. Mice received a simultaneous injection of pEGFP-N1 (25 μg) and pDsRed2-N1 (25 μg) by the hydrodynamics-based procedure (A) or sequential hydrodynamics-based injections of pEGFP-F (25 μg) followed by pDsRed2-N1 (25 μg) after a 4-h interval (B). The mice were euthanized 24 h after the first injection, and liver sections were prepared. The images shown are typical of those observed in several visual fields.

termediate which form stem-loop-structured siRNA (i.e., stem-loop-type). Comparative study revealed that both stem-loop- and tandem-type siRNA-expressing pDNAs were active in vivo, whereas the stem-loop-type pDNA produced more potent suppression than the tandem-type pDNAs (Fig. 1). This indicates that, despite the requirement of Dicer processing steps, stem-loop-structured siRNA is more suitable in vivo at least in the liver following the hydrodynamics-based delivery, although additional investigations are needed to determine the optimal siRNA-expressing vector involving modified loop sequences and functional elements in the vector construct.

Intravenous injection of pU6-stem21 by the hydrodynamics-based procedure resulted in significant suppression of the target transgene expression in organs including the liver, kidney, and lung (Fig. 2). Because the liver is the organ with the highest transgene expression level following the hydrodynamics-based procedure (Liu et al., 1999; Kobayashi et al., 2002), an obvious inhibitory effect was observed in the liver. Intramuscular delivery of pU6-stem21 also caused a dramatic reduction (Fig. 2). These results indicate that RNAi is achieved in vivo by siRNA-transcribing DNA templates in various somatic cells such as the kidney, lung, and muscle in addition to the liver, as shown in a report involving synthetic siRNA-derived RNAi in a variety of organs in mice (Lewis et al., 2002). Furthermore, we found a distinct dose-response in the RNAi-induced transgene suppression (Fig. 3). An apparent increase in *Pp*-Luc$^+$/*Rr*-Luc values in mice treated with the lowest dose of pU6-stem21 is probably due to a difference in the availability or stability of pGL3-control and pRL-SV40 in mice injected with 100 or 1 μg of pU6 vector. This speculation can be supported by the experimental data showing that injection of different amounts of pGL3-control and pRL-SV40 in a fixed ratio did not result in a constant *Pp*-Luc$^+$/*Rr*-Luc value (data not shown).

It was revealed that a reduction in transgene expression became apparent at day 1 after simultaneous injection and remained thereafter, whereas only a slight inhibition was obtained before this (Fig. 4). In addition, the transgene suppression determined at 6 h was limited to 50% inhibition at most, even in mice treated with an effector:target pDNA ratio of 10,000:1 (w/w) (Fig. 5). On the contrary, an effector:target pDNA ratio of approximately 33:1 or 3:1 (w/w) resulted in a very marked suppression when it was determined 3 days after injection (Fig. 3). These results suggest that it requires a specific period until the suppressive effect becomes apparent following simultaneous injection of effector and target pDNAs. We assumed two possible reasons for the delayed appearance of the transgene suppression. First, for cleavage of target mRNA, an injection of siRNA-expressing pDNA requires many steps, such as cellular uptake and nuclear localization of the injected pDNA, transcription of encoded RNA in the downstream of U6 promoter, transport of the RNA to the cytosol, processing by Dicer to produce functional siRNAs, and incorporation of the siRNAs to RISC, even if the hydrodynamics-based procedure produces rapid intracellular delivery of pDNA through the cellular membrane (Kobayashi et al., 2001, 2004). Second, since we introduced the target mRNA-expressing pDNA exogenously along with the effector pDNA, the expression of target mRNA was transient and the amount of intracellular mRNA varied with time. The promoters used in the present study, a virus-derived cytomegalovirus promoter and a human U6 promoter, were possibly different in their expression profiles, and the target mRNA should reach a maximum level earlier than the effector siRNA due to immediate inactivation of virus-derived promoter (Loser et al., 1998).

The duration of gene suppression is largely dependent on the rate of cell growth and the turnover of the targeted protein in actively dividing cell cultures. Since somatic cells like hepatocytes are not actively dividing, the duration of siRNA-mediated gene silencing in vivo might be governed by the activity of the siRNA-expressing vector and the stability of the functional siRNA as well as the lifespan of the targeted protein. The amount of actively transcribing target pDNA is supposed to decline over time partially in parallel with the amount of available siRNA-expressing pDNA following simultaneous injection of effector and target pDNAs. It might be possible that the observed 11-day persistence of transgene suppression does not represent the actual duration of inhibitory effect but is simply due to a significant inhibition achieved at an earlier time point (Fig. 4). Therefore, to estimate the duration of provision of active siRNA following siRNA-expressing pDNA injection, we performed sequential hydrodynamics-based injections of effector pDNA followed by target pDNAs. Transgene expression was markedly suppressed by 6-h or 1-day prior injection of pU6-stem21, but not by 4- or 11-day prior injection, indicating that the siRNA remained active and sufficient for transgene suppression for at least 1 day after siRNA-expressing pDNA injection under the present experimental conditions (Fig. 6). Since siRNA-expressing pDNA was delivered beforehand and probably had a sufficiently long period for the required processes, including the transcription and processing of targeted siRNA, the suppressive effect could be obtained as early as 6 h after target pDNA injection (Fig. 6; 6 h and 1 day). However, the degree of transgene suppression seemed to be lower compared with the result determined at day 1 after simultaneous injection as shown in Fig. 4.

To address these differences in the efficacy of transgene suppression between the ways of siRNA-expressing pDNA injection, we examined the localization of the transgene-expressing cells following the hydrodynamics-based procedure. It was found that a sequential delivery of the GFP- and DsRed-expressing pDNAs tended to give the green or the red

signals to separated cells (Fig. 7), indicating that the localization of transgene-expressing cells of the primary and the secondary pDNA injections by the hydrodynamics-based procedure was apparently different. Thus, it seems that, unlike the case of endogenous targets, simultaneous injection does not affect the transfection efficiency in terms of its suppressive effect since the effector and target pDNAs are supposed to be delivered to identical cells (Figs. 2–5). Moreover, the different hepatic localization of the effector and the target pDNAs, which were injected separately, accounts for the lower inhibitory effect in the sequential injection experiment shown in Fig. 6. In other words, suppression of transgene expression was obtained in only a fraction of the cells where both the siRNA-expressing pDNA and the target pDNAs were delivered, resulting in an apparently lower inhibition. This different localization of transgene positive cells further implies that a study of siRNA-mediated gene therapy in transgene-derived animal models for viral infections, in which hepatitis B, C, or D viral genomic DNA or RNA was introduced by the hydrodynamics-based procedure (Chang et al., 2001; McCaffrey et al., 2002b; Yang et al., 2002), should take the delivery efficiency into account.

In addition to their lower cost of production, vector-based approaches for induction of in vivo RNAi have a number of potential advantages including the possibility of sustained gene silencing and regulation of siRNA expression. The U6 promoter could be controlled with respect to its activity to transcribe RNAs by modification of the promoter to a tetracycline-responsive derivative (Ohkawa and Taira, 2000; Taira and Miyagishi, 2001). Xia et al. (2002) recently demonstrated successful RNAi induction via a Pol II, cytomegalovirus promoter-driven siRNA-expression system, indicating the possibility of tissue- or cell-selective induction of siRNA by regulation of the Pol II system. Although further studies are needed to improve the efficacy of siRNA-expressing vector, the present results provide useful information for future strategies for the induction of vector-based in vivo RNAi.

References

Brummelkamp TR, Bernards R, and Agami R (2002) A system for stable expression of short interfering RNAs in mammalian cells. *Science (Wash DC)* **296**:550–553.

Caplen NJ, Parrish S, Imani F, Fire A, and Morgan RA (2001) Specific inhibition of gene expression by small double-stranded RNAs in invertebrate and vertebrate systems. *Proc Natl Acad Sci USA* **98**:9742–9747.

Chang J, Sigal LJ, Lerro A, and Taylor J (2001) Replication of the human hepatitis delta virus genome is initiated in mouse hepatocytes following intravenous injection of naked DNA or RNA sequences. *J Virol* **75**:3469–3473.

Chiu YL and Rana TM (2002) RNAi in human cells: basic structural and functional features of small interfering RNA. *Mol Cell* **10**:549–561.

Dykxhoorn DM, Novina CD, and Sharp PA (2003) Killing the messenger: short RNAs that silence gene expression. *Nat Rev Mol Cell Biol* **4**:457–467.

Elbashir SM, Harborth J, Lendeckel W, Yalcin A, Weber K, and Tuschl T (2001) Duplexes of 21-nucleotide RNAs mediate RNA interference in cultured mammalian cells. *Nature (Lond)* **411**:494–498.

Hannon GJ (2002) RNA interference. *Nature (Lond)* **418**:244–251.

Hutvagner G and Zamore PD (2002) RNAi: nature abhors a double-strand. *Curr Opin Genet Dev* **12**:225–232.

Kawasaki H and Taira K (2003) Short hairpin type of dsRNAs that are controlled by tRNA(Val) promoter significantly induce RNAi-mediated gene silencing in the cytoplasm of human cells. *Nucleic Acids Res* **31**:700–707.

Kobayashi N, Kuramoto T, Chen S, Watanabe Y, and Takakura Y (2002) Therapeutic effect of intravenous interferon gene delivery with naked plasmid DNA in murine metastasis models. *Mol Ther* **6**:737–744.

Kobayashi N, Kuramoto T, Yamaoka K, Hashida M, and Takakura Y (2001) Hepatic uptake and gene expression mechanisms following intravenous administration of plasmid DNA by conventional and hydrodynamics-based procedures. *J Pharmacol Exp Ther* **297**:853–860.

Kobayashi N, Nishikawa M, Hirata K, and Takakura Y (2004) Hydrodynamics-based procedure involves transient hyperpermeability in the hepatic cellular membrane: implication of a nonspecific process in efficient intracellular gene delivery. *J Gene Med*, in press.

Lee NS, Dohjima T, Bauer G, Li H, Li MJ, Ehsani A, Salvaterra P, and Rossi J (2002) Expression of small interfering RNAs targeted against HIV-1 rev transcripts in human cells. *Nat Biotechnol* **20**:500–505.

Lewis DL, Hagstrom JE, Loomis AG, Wolff JA, and Herweijer H (2002) Efficient delivery of siRNA for inhibition of gene expression in postnatal mice. *Nat Genet* **32**:107–108.

Liu F, Song Y, and Liu D (1999) Hydrodynamics-based transfection in animals by systemic administration of plasmid DNA. *Gene Ther* **6**:1258–1266.

Loser P, Jennings GS, Strauss M, and Sandig V (1998) Reactivation of the previously silenced cytomegalovirus major immediate-early promoter in the mouse liver: involvement of NFkappaB. *J Virol* **72**:180–190.

Makimura H, Mizuno TM, Mastaitis JW, Agami R, and Mobbs CV (2002) Reducing hypothalamic AGRP by RNA interference increases metabolic rate and decreases body weight without influencing food intake. *BMC Neurosci* **3**:18.

McCaffrey AP, Meuse L, Pham TT, Conklin DS, Hannon GJ, and Kay MA (2002a) RNA interference in adult mice. *Nature (Lond)* **418**:38–39.

McCaffrey AP, Nakai H, Pandey K, Huang Z, Salazar FH, Xu H, Wieland SF, Marion PL, and Kay MA (2003) Inhibition of hepatitis B virus in mice by RNA interference. *Nat Biotechnol* **21**:639–644.

McCaffrey AP, Ohashi K, Meuse L, Shen S, Lancaster AM, Lukavsky PJ, Sarnow P, and Kay MA (2002b) Determinants of hepatitis C translational initiation in vitro, in cultured cells and mice. *Mol Ther* **5**:676–684.

McManus MT, Petersen CP, Haines BB, Chen J, and Sharp PA (2002) Gene silencing using micro-RNA designed hairpins. *RNA (NY)* **8**:842–850.

Miyagishi M and Taira K (2002) U6 promoter-driven siRNAs with four uridine 3′ overhangs efficiently suppress targeted gene expression in mammalian cells. *Nat Biotechnol* **20**:497–500.

Miyagishi M and Taira K (2003) Expression of siRNA from a pol III promoter in mammalian cells, in *Perspectives in Gene Expression* (Appasani K ed) pp 361–376, The Eaton Publishers, Westboro, MA.

Ohkawa J and Taira K (2000) Control of the functional activity of an antisense RNA by a tetracycline-responsive derivative of the human U6 snRNA promoter. *Hum Gene Ther* **11**:577–585.

Paddison PJ, Caudy AA, Bernstein E, Hannon GJ, and Conklin DS (2002a) Short hairpin RNAs (shRNAs) induce sequence-specific silencing in mammalian cells. *Genes Dev* **16**:948–958.

Paddison PJ, Caudy AA, and Hannon GJ (2002b) Stable suppression of gene expression by RNAi in mammalian cells. *Proc Natl Acad Sci USA* **99**:1443–1448.

Paul CP, Good PD, Winer I, and Engelke DR (2002) Effective expression of small interfering RNA in human cells. *Nat Biotechnol* **20**:505–508.

Reich SJ, Fosnot J, Kuroki A, Tang W, Yang X, Maguire AM, Bennett J, and Tolentino MJ (2003) Small interfering RNA (siRNA) targeting VEGF effectively inhibits ocular neovascularization in a mouse model. *Mol Vis* **9**:210–216.

Song E, Lee SK, Wang J, Ince N, Ouyang N, Min J, Chen J, Shankar P, and Lieberman J (2003) RNA interference targeting Fas protects mice from fulminant hepatitis. *Nat Med* **9**:347–351.

Sorensen DR, Leirdal M, and Sioud M (2003) Gene silencing by systemic delivery of synthetic siRNAs in adult mice. *J Mol Biol* **327**:761–766.

Stein P, Svoboda P, Anger M, and Schultz RM (2003) RNAi: mammalian oocytes do it without RNA-dependent RNA polymerase. *RNA* **9**:187–192.

Sui G, Soohoo C, Affar el B, Gay F, Shi Y, and Forrester WC (2002) A DNA vector-based RNAi technology to suppress gene expression in mammalian cells. *Proc Natl Acad Sci USA* **99**:5515–5520.

Svoboda P, Stein P, and Schultz RM (2001) RNAi in mouse oocytes and preimplantation embryos: effectiveness of hairpin dsRNA. *Biochem Biophys Res Commun* **287**:1099–1104.

Taira K and Miyagishi M (2001) Technology Licensing Organization of Tokyo University (CASTI), assignee. siRNA expression system and method for producing functional gene knock-down cell using the system. Japanese Patent Application, 2001–363385.

Tavernarakis N, Wang SL, Dorovkov M, Ryazanov A, and Driscoll M (2000) Heritable and inducible genetic interference by double-stranded RNA encoded by transgenes. *Nat Genet* **24**:180–183.

Verma UN, Surabhi RM, Schmaltieg A, Becerra C, and Gaynor RB (2003) Small interfering RNAs directed against beta-catenin inhibit the in vitro and in vivo growth of colon cancer cells. *Clin Cancer Res* **9**:1291–1300.

Xia H, Mao Q, Paulson HL, and Davidson BL (2002) siRNA-mediated gene silencing in vitro and in vivo. *Nat Biotechnol* **20**:1006–1010.

Yang PL, Althage A, Chung J, and Chisari FV (2002) Hydrodynamic injection of viral DNA: a mouse model of acute hepatitis B virus infection. *Proc Natl Acad Sci USA* **99**:13825–13830.

Yu JY, DeRuiter SL, and Turner DL (2002) RNA interference by expression of short-interfering RNAs and hairpin RNAs in mammalian cells. *Proc Natl Acad Sci USA* **99**:6047–6052.

Zamore PD (2002) Ancient pathways programmed by small RNAs. *Science (Wash DC)* **296**:1265–1269.

Zeng Y and Cullen BR (2002) RNA interference in human cells is restricted to the cytoplasm. *RNA* **8**:855–860.

Address correspondence to: Yoshinobu Takakura, Department of Biopharmaceutics and Drug Metabolism, Graduate School of Pharmaceutical Sciences, Kyoto University, Sakyo-ku, Kyoto 606-8501, Japan. E-mail: takakura@pharm.kyoto-u.ac.jp

THE JOURNAL OF GENE MEDICINE
J Gene Med 2004; 6: 584–592.
Published online 18 February 2004 in Wiley InterScience (www.interscience.wiley.com). DOI: 10.1002/jgm.541

RESEARCH ARTICLE

Hydrodynamics-based procedure involves transient hyperpermeability in the hepatic cellular membrane: implication of a nonspecific process in efficient intracellular gene delivery

Naoki Kobayashi
Makiya Nishikawa
Kazuhiro Hirata
Yoshinobu Takakura*

Department of Biopharmaceutics and Drug Metabolism, Graduate School of Pharmaceutical Sciences, Kyoto University, Sakyo-ku, Kyoto 606-8501, Japan

*Correspondence to:
Yoshinobu Takakura, Department of Biopharmaceutics and Drug Metabolism, Graduate School of Pharmaceutical Sciences, Kyoto University, Sakyo-ku, Kyoto 606-8501, Japan.
E-mail:
takakura@pharm.kyoto-u.ac.jp

Received: 5 September 2003
Revised: 5 December 2003
Accepted: 16 December 2003

Abstract

Background The mechanisms underlying the efficient gene transfer by a large-volume and high-speed intravenous injection of naked plasmid DNA (pDNA), a so-called hydrodynamics-based procedure, remain unclear and require further investigation. In this report, we have investigated possible mechanisms for the intracellular transport of naked pDNA by this procedure.

Methods Propidium iodide (PI), a fluorescent indicator for cell membrane integrity, and luciferase- or green fluorescent protein (GFP)-expressing pDNA were injected into mice by the hydrodynamics-based procedure.

Results PI was efficiently taken up by hepatocytes which appeared to be viable following the hydrodynamics-based procedure. Pre-expressed GFP in the cytosol was rapidly eliminated from the hepatocytes by a large-volume injection of saline. The profiles of plasma ALT and AST showed a steady decline with the highest values observed immediately after the hydrodynamics-based procedure. These results suggest that the hydrodynamics-based procedure produces a transient increase in the permeability of the cell membrane. The cellular uptake process appeared nonspecific, since simultaneous injection of an excess of empty vector did not affect the transgene expression. Sequential injections of a large volume of pDNA-free saline followed by naked pDNA in a normal volume revealed that the increase in membrane permeability was transient, with a return to normal conditions within 30 min. Transgene expression was observed in hepatocyte cultures isolated 10 min after pDNA delivery and in the liver as early as 10 min after luciferase-expressing RNA delivery, indicating that pDNA delivered immediately by the hydrodynamics-based procedure has the potential to produce successful transgene expression.

Conclusions These findings suggest that the mechanism for the hydrodynamics-based gene transfer would involve in part the direct cytosolic delivery of pDNA through the cell membrane due to transiently increased permeability. Copyright © 2004 John Wiley & Sons, Ltd.

Keywords hydrodynamics-based procedure; plasmid DNA; membrane permeability; gene delivery

Introduction

Nonviral gene delivery, which represents a promising *in vivo* gene transfer strategy due to its safety and versatility, has problems associated with the limited efficacy of transgene expression. Various physical or chemical approaches, such as electroporation, gene gun, and complex formation with cationic lipids or polymers, have been studied and developed to improve transgene expression efficacy and the target cell specificity of plasmid DNA (pDNA)-based nonviral gene transfer [1,2]. While these approaches have resulted in a relatively improved efficacy, current nonviral gene delivery systems are likely to require further improvements before their successful application to clinical gene therapy.

Hydrodynamics-based gene delivery, involving a large-volume and high-speed intravenous injection of naked pDNA, gives a significantly high level of transgene expression in the liver and other major organs [3,4]. This procedure has been used very frequently as a simple and convenient *in vivo* transfection method [5–17]. Furthermore, this method of gene transfer allows naked pDNA to be sufficiently effective to obtain therapeutic levels of target transgene products [6,9,10,15–17]. The principle of the hydrodynamics-based procedure could be applicable to an organ-restricted gene delivery method; i.e. targeting to the organs such as the liver, the kidney and the hindlimb muscles by injection via a suitable vein or artery with transient occlusion of the outflow as demonstrated previously [18–23]. In actual fact, Eastman *et al.* [24] recently reported the catheter-mediated hydrodynamics-based delivery of pDNA using isolated rabbit liver.

In spite of the frequent use of the hydrodynamics-based procedure in functional studies of therapeutic genes or DNA elements, little is known about the mechanisms underlying efficient gene transfer by this procedure. Liu *et al.* [3] demonstrated that a rapid injection and a large volume of pDNA solution were required to obtain a high level of transgene expression, indicating that a high blood pressure was the most critical factor for the gene transfer efficiency, and proposed that pDNA might be transferred inside the liver cells by the 'hydrodynamic' process. In contrast, it was hypothesized that the cellular uptake mechanism of naked pDNA injected by the hydrodynamics-based procedure involved a specific process such as receptor-mediated endocytosis [25]. In our previous study, involving the *in vivo* disposition of naked pDNA following the normal or the hydrodynamics-based procedure, in support of the speculation of Liu and colleagues, we demonstrated that the hepatic uptake process appeared nonspecific, being different from that involved in the normal intravenous injection of naked pDNA [26]. Since the cellular uptake mechanisms are still controversial, they need to be better understood for further application of the hydrodynamics-based procedure for both therapeutic applications and basic studies. In the present study, we have investigated a possible mechanism for hydrodynamics-based gene transfer and suggest that it would involve in part a nonspecific process via a cell membrane which becomes permeable for a short period.

Materials and methods

Chemicals

Propidium iodide (PI), type I-A collagenase, type II-S soybean trypsin inhibitor, and William's medium E were purchased from Sigma (St. Louis, MO, USA). Type I rat tail collagen and ITS(+) were purchased from BD Biosciences (San Jose, CA, USA). Injectable saline solution purchased from Otsuka (Tokyo, Japan) was used as the vehicle for plasmid DNA (pDNA) or PI injection in all the experiments. All other chemicals used were of the highest purity available.

Plasmid DNA

pEGFP-N1 encoding enhanced green fluorescent protein (EGFP) and pEGFP-F encoding farnesylated EGFP, that remain bounds to the plasma membrane in both living and fixed cells [27,28], were purchased from BD Biosciences Clontech (Palo Alto, CA, USA). pcDNA3 vector was purchased from Invitrogen (Carlsbad, CA, USA). pCMV-Luc was constructed by insertion of the Hind III/Xba I firefly luciferase cDNA fragment from pGL3-control (Promega, Madison, WI, USA) into the polylinker of pcDNA3 as described earlier [29]. pRLIL-3'NC containing sea pansy luciferase and firefly luciferase genes was kindly provided by Professor Kunitada Shimotohno (Department of Viral Oncology, Institute for Virus Research, Kyoto University, Japan). Each pDNA was amplified in the DH5α strain of *Escherichia coli* and purified using a QIAGEN Endofree Plasmid Giga kit (QIAGEN GmbH, Hilden, Germany).

RNA synthesis

Luciferase-expressing RNA was synthesized by *in vitro* transcription using a MEGAscript T7 kit (Ambion, Austin, TX, USA) according to the manufacturer's instructions. Hind III-linearized pRLIL-3'NC was used as a template. The transcribed RNA was treated with DNase I to minimize template contamination and purified by a standard phenol/chloroform extraction and isopropanol precipitation method. Since no cap analogs were added to the reaction mixture, the transcribed RNA could produce only the internal ribosomal entry site (IRES)-dependent expression of firefly luciferase. The synthesized RNA was dissolved in saline (Otsuka) just before intravenous injection to mice.

Mice and intravenous injection

Four-week-old female ddY mice (approximately 20 g body weight), purchased from Shizuoka Agricultural Cooperative Association for Laboratory Animals (Shizuoka, Japan), were used for all experiments. Mice received a tail vein injection in a volume of 100 µl (otherwise mentioned) or 1.6 ml for the normal or the hydrodynamics-based procedure, respectively. The tail vein injection was performed over less than 5 s using a 26-gauge needle for both procedures.

Confocal microscopic study of liver sections

Mice were euthanized by cutting the vena cava at the described time and the liver was gently infused with 5 ml saline through the portal vein to remove remaining blood. The liver was then embedded in Tissue-Tek OCT embedding compound (Sakura Finetechnical Co., Ltd., Tokyo, Japan), frozen in liquid nitrogen and stored in 2-methylbutanol at −80 °C. Frozen liver sections were made, 8 µm in thickness, using a cryostat (Jung Frigocut 2800E; Leica Microsystems AG, Wetzlar, Germany) by the routine procedure. With some exceptions, the sections were directly subjected to confocal microscopic observation (MRC-1024; BioRad, Hercules, CA, USA) without any fixation, since the fixation step caused a massive loss of GFP due to immediate dissolution in the fixation buffer in our preliminary experiments. In the case of mice injected with PI alone, their liver sections were fixed with Mildform 20N (8% paraformaldehyde; Wako, Osaka, Japan) for 4 min at 4 °C followed by confocal microscopic observation.

Luciferase assay

To determine luciferase activities, the organs including the liver, kidney, lung, spleen and heart were excised and homogenized in 5 ml/g (liver) or 4 ml/g (other organs) of lysis buffer (0.1 M Tris, 0.05% Triton X-100, 2 mM EDTA, pH 7.8). The homogenate was subjected to three cycles of freezing (−190 °C) and thawing (37 °C) and centrifuged at 10 000 *g* for 10 min at 4 °C. Then, appropriately diluted supernatant was mixed with luciferase assay buffer (Picagene, Toyo Ink, Tokyo, Japan) and the chemiluminescence produced was measured in a luminometer (Lumat LB 9507; EG & G Berthold, Bad Wildbad, Germany).

Determination of plasma transaminase activities

At the indicated time points after large-volume injection of saline, blood was collected from the vena cava by heparinized syringe and plasma was obtained by centrifugation. Alanine aminotransferase (ALT/GPT) and aspartate aminotransferase (AST/GOT) activities in the plasma were determined by commercially available test reagents (GPT-UV test Wako and GOT-UV test Wako, respectively; Wako, Osaka, Japan). Normal values were determined using the blood obtained from age-matched, untreated mice. We also confirmed the mice did not show any increase in their plasma ALT and AST following an intravenous injection of a small volume of saline (data not shown).

Isolation and culture of primary hepatocytes

The hepatocytes were isolated by collagenase digestion followed by differential centrifugation according to a previous report [30]. Briefly, at 10 min after intravenous injection of either pCMV-Luc, pEGFP-N1 or pDNA-free saline by the hydrodynamics-based procedure, mice were euthanized and the liver was perfused via the portal vein with preperfusion buffer (Ca^{2+}- and Mg^{2+}-free HEPES buffer, pH 7.2) and then with HEPES buffer (pH 7.5) containing 5 mM $CaCl_2$, 0.005% (w/v) soybean trypsin inhibitor and 0.05% (w/v) collagenase. The liver cells dispersed in ice-cold Hank's-HEPES buffer (pH 7.2) were incubated at 37 °C for 10 min followed by filtration through a Farcon® 100-µm nylon cell strainer (Becton Dickinson, Franklin Lakes, NJ, USA) to remove aggregates of dying cells and then fractionated into hepatocytes and nonparenchymal cells by differential centrifugation. The hepatocytes were suspended in William's medium E supplemented with ITS(+) and penicillin/streptomycin/L-glutamine and seeded on collagen-coated 12-well plates with/without cover slips at a density of 2×10^5 cells/well. After culturing for 24 h at 37 °C, the cells were washed twice with phosphate-buffered saline (PBS) and then fixed with 4% paraformaldehyde for confocal microscopic observation or directly collected by scraping for luciferase assay.

Results

Increase in cell membrane permeability of hepatocytes by the hydrodynamics-based procedure

To examine whether the permeability of the hepatocyte cellular membrane was affected by the hydrodynamics-based procedure, we injected mice intravenously with propidium iodide (PI), a fluorescent substance binding to double-stranded DNA, which is not supposed to cross the plasma membrane of viable cells. Figure 1 shows the liver sections of mice receiving PI by the normal or the hydrodynamics-based procedure. While none of the liver cells were stained with PI following the normal procedure, the hydrodynamics-based procedure caused

an efficient intracellular delivery of PI at 10 min after injection (Figures 1A and 1B). However, a substantial reduction in the fluorescent intensity of nuclear PI staining was observed in a large portion of the hepatocytes at 6 h after the hydrodynamics-based PI injection (data not shown). Simultaneous injection of PI and pEGFP-N1 by the hydrodynamics-based procedure resulted in a significant level of transgene expression without overlap of red and green signals (Figures 1D), indicating that PI-positive cells after a longer period were necrotic or apoptotic with no potentials to express transgene.

To obtain further information on the increased cell membrane permeability of the hepatocytes, we next examined the efflux of GFP from the hepatocytes following the hydrodynamics-based procedure. Because GFP is highly water-soluble and present unbound in the cytosol, it is likely to diffuse from the cytoplasm through the permeable cell membrane. As is evident in Figures 2A and 2B, fluorescent signals of GFP expressed beforehand in the liver were apparently eliminated by the second hydrodynamics-based saline injection. To examine the possibility if the second hydrodynamics-based injection to the same animals might cause significant damage to mouse liver, resulting in the decreased level of GFP, we performed the same experiments using pEGFP-F which encodes a modified form of EGFP that remains bound to the inner face of plasma membrane [27,28]. As a result, the amount of EGFP-F was not significantly affected by the

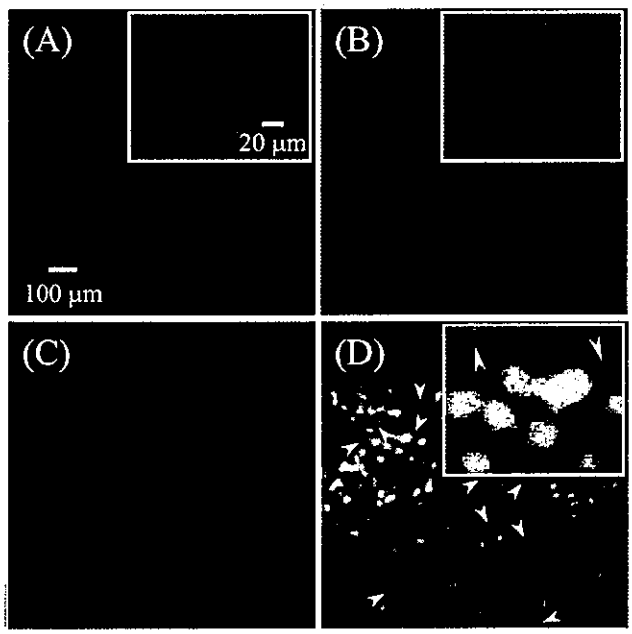

Figure 1. Confocal microscopic images of the liver following an intravenous injection of PI with/without GFP-expressing pDNA. Mice injected with PI (40 μg) by the normal (A) or the hydrodynamics-based (B) procedure were euthanized at 10 min and liver sections were made. Mice that received a simultaneous injection of PI (100 μg) and pEGFP-N1 (25 μg) by the normal (C) or the hydrodynamics-based (D) procedure were euthanized at 6 h and liver sections were made. The images shown are typical of those observed in several visual fields of three mice. Arrowheads indicate the PI-positive cells at 6 h after injection (D). Red: PI; green: GFP

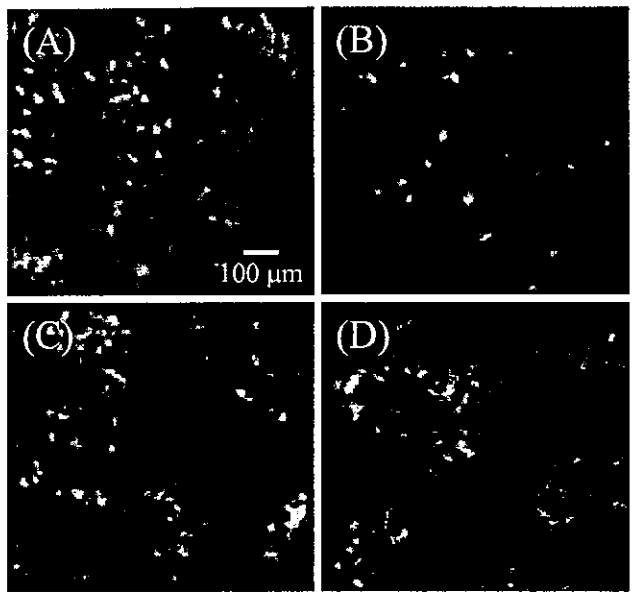

Figure 2. Elimination of pre-expressed GFP in the liver by a large-volume injection of saline. Mice injected beforehand with pEGFP-N1 (25 μg) (A, B) or pEGFP-F (25 μg) (C, D) by the hydrodynamics-based procedure were subjected to a large-volume intravenous injection of saline (1.6 ml) (B, D) or no treatment (A, C) at 6 h. Ten minutes after a pDNA-free saline injection, mice were euthanized and liver sections were made. The images shown are typical of those observed in several visual fields of three mice

second hydrodynamics-based saline injection (Figures 2C and 2D). This was confirmed by an *in vitro* assay where expressed EGFP-F but not EGFP remained within COS-7 cells following membrane permeabilization by Triton X-100 treatment (data not shown). A quantitative analysis by similar experiments using pCMV-Luc, where we did not observe any differences in luciferase activities in the liver between mice with or without the second hydrodynamics-based injection of saline (data not shown), further suggests that the decrease in GFP level is not simply due to a significant damage or denaturation of the expressed GFP. These results further confirm the increased permeability of the hepatocyte cellular membrane.

Time-course of plasma transaminase activities following the hydrodynamics-based procedure

The hepatic enzymes, alanine aminotransferase (ALT) and aspartate aminotransferase (AST), are frequently used as indicators of liver damage. It has been reported that the hydrodynamics-based procedure caused transient liver damage with high serum ALT and AST levels, which rapidly returned to normal in a few days [3,16,31]. We assumed that, similar to the case of GFP effusion shown in Figure 2, the high levels of ALT and AST detected were attributed to release from the hepatocytes when the cellular membrane was transiently rendered permeable by the hydrodynamics-based procedure. Figure 3 shows the plasma concentration profiles of ALT and AST following

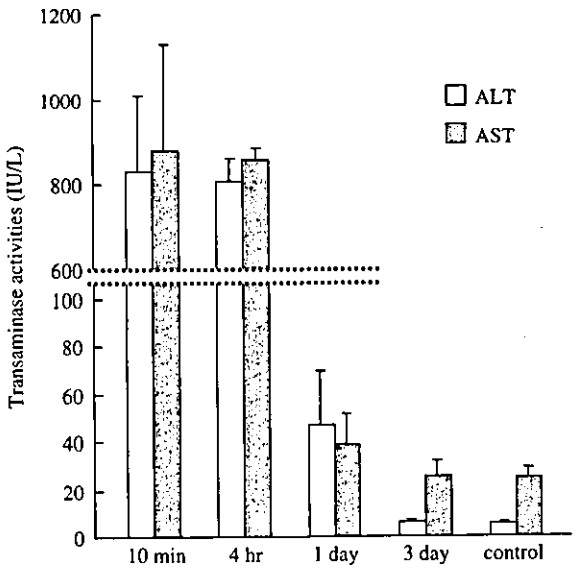

Figure 3. Profiles of plasma transaminase activities following a large-volume injection of saline into mice. Mice received a large-volume intravenous injection of saline (1.6 ml) and blood was collected at the indicated times. Plasma ALT and AST activities were determined. Control represents age-matched, untreated mice. The results are expressed as the mean ± S.D. (n = 3)

a large-volume injection of saline. As expected, the highest values for plasma ALT and AST were detected immediately after injection, i.e. at 10 min, when the large volume of injected saline should dilute the plasma, and, then, these enzyme levels decreased gradually, returning to normal within 3 days (Figure 3). Although it cannot be excluded at this moment that the high levels of ALT and AST observed following the hydrodynamics-based procedure were solely due to cell death, these facts further support the transient increase in the permeability of the hepatocyte cellular membrane.

Competitive effect of excess sham pDNA on transgene expression by the hydrodynamics-based procedure

To discuss the nonspecificity in the process of pDNA cellular uptake following the hydrodynamics-based procedure, we performed a competitive study of transgene expression by a simultaneous injection of pCMV-Luc and an excess of empty vector, pcDNA3. As shown in Figure 4A, transgene expression reached a plateau at 5 μg pCMV-Luc, consistent with the previous report [3]. The transgene expression level in the liver was not affected by simultaneous injection of a saturable amount of pcDNA3 (Figure 4B), suggesting that the hydrodynamics-based gene transfer was a nonspecific process. We also confirmed that the pDNA dose employed in the present study (0.2 μg/mouse) was in the linear region; reduction of the dose caused a substantial fall in transgene expression (Figure 4A).

Duration of the increased membrane permeability following the hydrodynamics-based procedure

To examine how long the hydrodynamics-based procedure maintains the increased permeability of the cell membrane, we performed sequential intravenous injections of a large volume of pDNA-free saline followed by a normal injection of naked pDNA at various time intervals. Figure 5 shows the effect of the time intervals of the two sequential injections on the transgene expression of pCMV-Luc. A prior intravenous injection of a large volume of saline could potentiate a subsequent normal intravenous injection of naked pDNA to produce a significantly high level of luciferase expression in the liver, while no transgene expression was obtained by naked pDNA injection alone in a normal volume (Figure 5). The level of luciferase activity was negatively correlated with the time intervals and marked transgene expression could be obtained up to 15 to 30 min. This phenomenon was also observed in all the other organs tested. Among them, the effect of a prior large-volume injection seemed the most sustained in the lung.

Potential of initially delivered pDNA and RNA for significant transgene expression following the hydrodynamics-based procedure

We examined if a population of intracellular pDNA delivered immediately after injection, during which the increased permeability of the cell membrane appeared to be maintained, could result in a significant level of transgene expression. As shown in Figure 6A, GFP-expressing cells were observed in the hepatocyte culture isolated 10 min after the hydrodynamics-based delivery of pEGFP-N1. Also, a high level of luciferase activity was detected in the cells isolated from mice following the hydrodynamics-based pCMV-Luc injection (Figure 6C). The hepatocytes isolated from saline-treated mice did not show either a GFP signal or luciferase activity (Figures 6B and 6C).

To further provide evidence of the nucleic acid delivered intracellularly immediately after the hydrodynamics-based procedure, we examined the transgene expression at various time points following an intravenous injection of luciferase-expressing RNA. As shown in Figure 7, a significant level of luciferase activity was obtained in the liver as early as 10 min after the hydrodynamics-based procedure. It was confirmed that the produced luciferase activity was derived from the injected RNA not the contaminated template DNA, since RNase A treatment before injection led to a blank level of transgene expression.

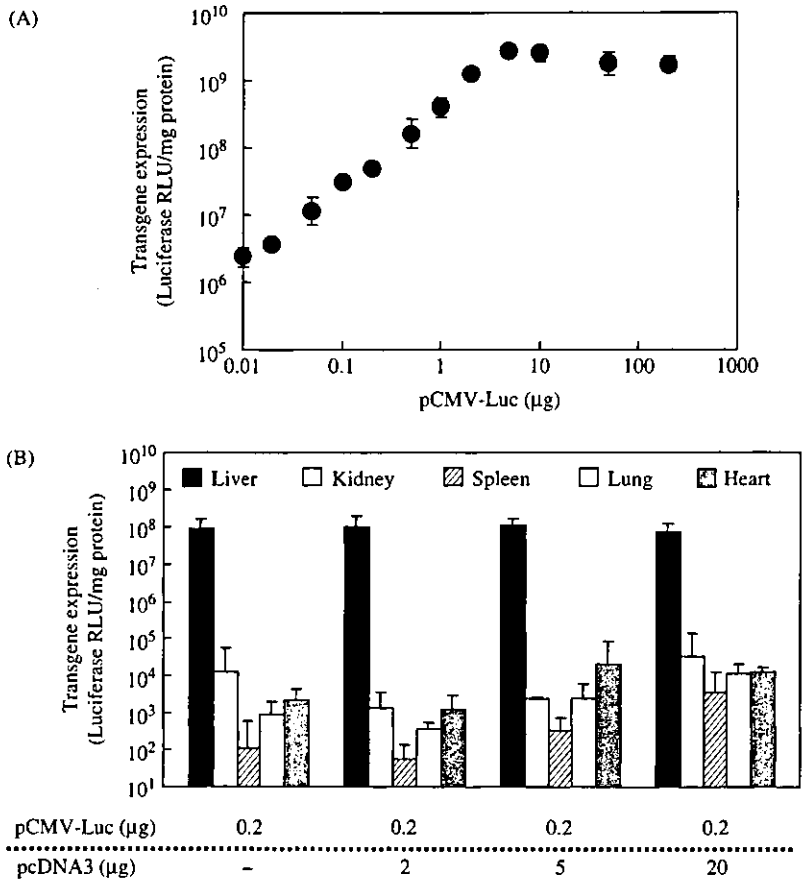

Figure 4. Effect of simultaneous injection of excess sham pDNA on transgene expression by pCMV-Luc following the hydrodynamics-based procedure. Mice received an intravenous injection of various amounts of pCMV-Luc (0.01–200 μg) (A) or a simultaneous injection of pCMV-Luc (0.2 μg) and 10- to 100-fold doses of pcDNA3 (B) by the hydrodynamics-based procedure. At 6 h after injection, mice were euthanized and the luciferase activities in organs were determined. The results are expressed as the mean ± S.D. of at least three mice

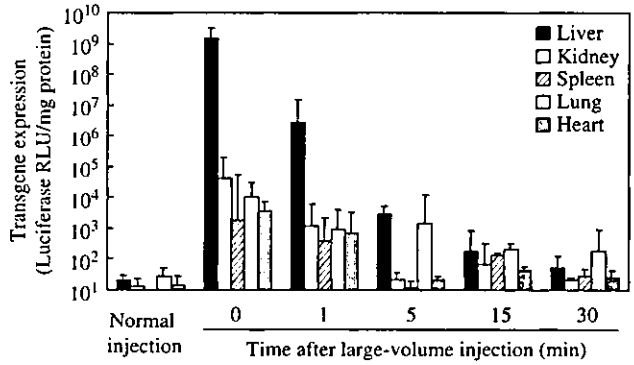

Figure 5. Effect of time interval between a prior large-volume injection of saline and a subsequent normal intravenous injection of pCMV-Luc on transgene expression. Mice received a large-volume intravenous injection of saline (1.6 ml) and, subsequently at the indicated times, an intravenous injection of naked pCMV-Luc (20 μg/mouse) in a normal volume (50 μl). The time interval of 0 min means pCMV-Luc injection by the hydrodynamics-based procedure. The normal injection means a pCMV-Luc injection (20 μg in 50 μl) without any large-volume injection. At 6 h after pDNA injection, mice were euthanized and the luciferase activities in organs were determined. The results are expressed as the mean ± S.D. of at least three mice

Discussion

The hydrodynamics-based gene delivery has been gaining much attention recently and is used very frequently as a simple and convenient efficient *in vivo* transfection method. Following the first reports of the large-volume injection [3,4], Budker *et al.* [25] hypothesized that the cellular uptake mechanism of naked pDNA involved an active, receptor-mediated process. Their hypothesis was prompted mainly by the observations that pDNA administered by the hydrodynamics-based procedure was present around hepatocytes immediately after injection but was internal in hepatocytes at 1 h after injection and that co-injection of excess polyanions inhibited pDNA uptake and expression. In addition, Lecocq *et al.* [32] demonstrated in a subcellular distribution study using differential centrifugation methods that ^{35}S-labeled pDNA remained bound to the outside surface of the plasma membrane for at least 1 h after the hydrodynamics-based procedure, supporting the hypothesis that pDNA was internalized slowly via a specific mechanism. However, in agreement with a notion of a 'hydrodynamics-based' process proposed by Liu and colleagues [3], we have demonstrated that the cellular uptake process

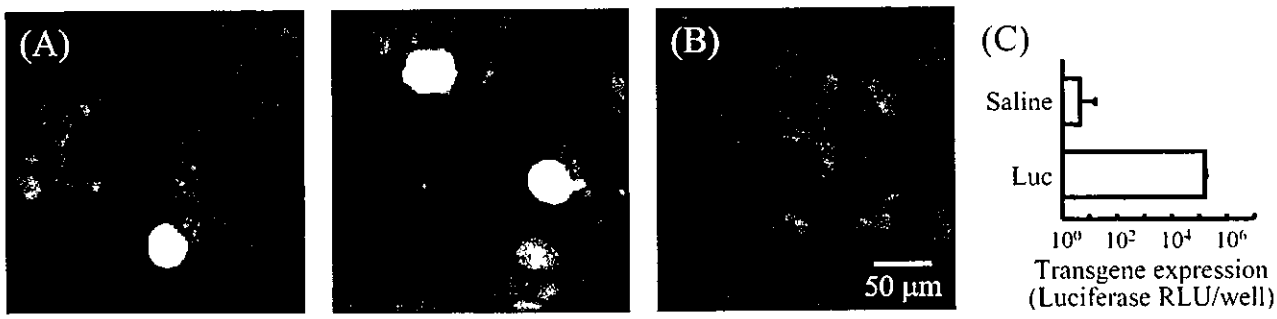

Figure 6. Transgene expression in primary hepatocytes isolated immediately after gene delivery by the hydrodynamics-based procedure. Ten minutes after intravenous injection of either pEGFP-N1 (25 μg), pCMV-Luc (25 μg) or pDNA-free saline by the hydrodynamics-based procedure, mice were euthanized and the hepatocytes were isolated as described in 'Materials and methods'. After 24 h culture, confocal microscopic observation of the cells from pEGFP-N1-injected mice (A) or saline-injected mice (B) was performed and luciferase activities were determined (C). The images shown are typical of those observed in several visual fields. The luciferase activities are expressed as the mean ± S.D. (n = 3)

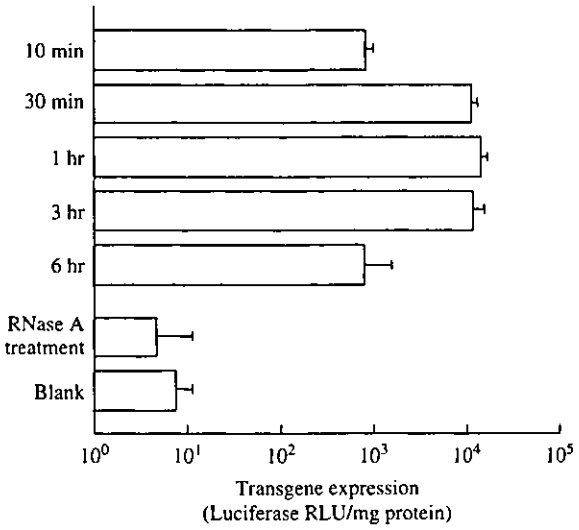

Figure 7. Transgene expression following luciferase-expressing RNA delivery by the hydrodynamics-based procedure. Mice received an intravenous injection of IRES-dependent luciferase-expressing RNA (25 μg) transcribed *in vitro* as described in 'Materials and methods' by the hydrodynamics-based procedure. Mice were euthanized at the indicated time point and the luciferase activities in the liver were determined. For a group of mice, the same RNA (25 μg) was treated with RNase A (15 μg/ml) at 37 °C for 15 min before injection. The results are expressed as the mean ± S.D. of three mice

involved in the hydrodynamics-based procedure appears to be nonspecific, since neither the hepatic uptake nor the transgene expression was inhibited by prior administration of polyanions, including poly I, dextran sulfate and heparin [26]. This was supported by the fact that significant hepatic uptake of bovine serum albumin and immunoglobulin G was observed after the hydrodynamics-based procedure [26]. The mechanisms underlying efficient gene transfer by the hydrodynamics-based procedure have not been clarified yet and must be better understood for further applications including gene therapy.

In the present study, we have investigated further the possible mechanisms, which have been controversial so far, governing hydrodynamics-based intracellular gene delivery. PI was effectively incorporated by the liver cells following the hydrodynamics-based procedure (Figure 1B). GFP expressed beforehand and accumulated internally in the cytosol was dramatically eliminated from the hepatocytes following a large-volume injection of saline (Figure 2). These results suggest a facilitated permeation of PI and GFP through the cell membrane, since PI and GFP are not supposed to cross the plasma membrane of viable cells. Contrary to our finding using PI, Budker *et al.* [25] previously observed that injection of a membrane-impermeable dye, TOTO-1, did not lead to nuclear fluorescence in liver cells. This might be accounted for by some differences in the experimental conditions. At least 10% of hepatocytes could be estimated PI-positive at 10 min (Figure 1B). Since Herweijer *et al.* [33] reported that the necrotic areas were less than 1% of the liver following the hydrodynamics-based procedure, all the PI-positive cells observed were not likely to be dead cells. Accordingly, it could be hypothesized that the time-dependent elimination of PI intensity might be a result of efflux or metabolism of PI by viable cells. The fact that only a few cells (estimated approximately 1%) remained PI-positive for a longer period without ability to express GFP further supports this hypothesis. A farnesylated GFP (EGFP-F), a membrane-bound modified form of GFP, was not eliminated by the second large-volume injection of saline (Figures 2C and 2D) and a similar result was obtained in the assay using luciferase (data not shown). While both EGFP and luciferase are supposed cytosolic proteins, the well-known higher water-solubility of EGFP might account for the differences, although the detailed mechanism is unclear. Taken together, it was suggested that the apparent increased permeability of the cell membrane was not simply attributed to cell death or severe cellular damage caused by the invasive nature of the large-volume injection itself.

Nonspecificity in the cellular uptake process of pDNA was further confirmed by a competitive study. A saturable amount of empty vector did not inhibit transgene expression in the liver following the hydrodynamics-based procedure (Figure 4B). In addition, our dose-response study suggests that the transgene expression